Arabian Journal of Chemistry (2012) **5**, 397–417

King Saud University

Arabian Journal of Chemistry

www.ksu.edu.sa
www.sciencedirect.com

REVIEW

1st Nano Update

Microemulsion method: A novel route to synthesize organic and inorganic nanomaterials

Maqsood Ahmad Malik [a,*], Mohammad Younus Wani [b], Mohd Ali Hashim [a]

[a] *Department of Chemical Engineering, University Malaya, 50603 Kuala Lumpur, Malaysia*
[b] *Center for Interdisciplinary Research in Basic Sciences, Jamia Millia Islamia (Central University), New Delhi 110025, India*

Received 1 September 2010; accepted 27 September 2010
Available online 2 October 2010

KEYWORDS

Microemulsions;
Nanoparticle;
Nanoparticle synthesis

Abstract Synthesis of nanoparticles by microemulsion method is an area of considerable current interest. Since the discovery of microemulsions, they have attained increasing significance both in basic research and in different industrial fields. Due to their unique properties, namely, ultralow interfacial tension, large interfacial area, thermodynamic stability and the ability to solubilize otherwise immiscible liquids. The uses and applications of microemulsions are numerous in chemical and biological fields. The nanoparticles not only are of basic scientific interest, but also have resulted in important technological applications, such as catalysts, high-performance ceramic materials, microelectronic devices, high-density magnetic recording and drug delivery. The microemulsion technique promises to be one of the versatile preparation method which enables to control the particle properties such as mechanisms of particle size control, geometry, morphology, homogeneity and surface area. This review aims to give a vivid look on the use of microemulsions for synthesizing and controlling the grain size and morphology of the nanoparticles and at the same time will summarize some recent works carried out in the synthesis of organic and inorganic nanoparticles by this method.

* Corresponding author. Tel.: +6 0147223740.
E-mail address: maqsoodchem@gmail.com (M.A. Malik).

Peer-review under responsibility of King Saud University.
doi:10.1016/j.arabjc.2010.09.027

Production and hosting by Elsevier

Contents

1. Introduction

Field of nanotechnology come out from the different scientific fields like physical, chemical, biological and engineering sciences where novel techniques are being developed to control single atoms and molecules. Nanoparticle in nanotechnology is defined as a small object that behaves as a whole unit in terms of its transport properties and potential application. Nanoparticles of either simple or composite nature are important materials in the development of novel nanodevices which can be used in numerous physical, biological, biomedical and pharmaceutical applications (Chan et al., 2002; Brigger et al., 2002; Sondi et al., 2000). Nanoparticles and nanostructured materials have been fascinating the world of science for decades due to their use in catalysis, photography, photonics, electronics, labeling, imaging, sensing and surface enhanced Raman scattering. They are among the most challenging areas of current scientific and technological research because of interesting changes in their optical, magnetic, catalytic, electrical and drug delivery properties accompanied with improved physical properties like mechanical hardness, thermal stability or chemical passivity. Many optical properties of nanoparticles often differ drastically from those of the single crystals with the same chemical composition. At nanometer size, crystallites are influenced by the presence of significant number of surface atoms and by the quantum confinement effect of the electronic states and this influences the property of nanomaterials as compared to their bulk phases. The properties of matter within this scale are significantly different from individual atoms or molecules and from bulk materials (Dong-Hwang and Szu-Han, 2003). These inorganic and organic nanomaterials have been synthesized by a variety of physical and chemical methods like chemical reduction methods (Zaheer et al., 2010; Ahmad et al., 2010; Chou and Ren, 2000; Nersisyan et al., 2003; Nickel et al., 2000; Sun and Xia, 2002; Sileikaite et al., 2006), thermal methods (Sun and Luo, 2005), irradiation methods (Shao and Yao, 2006; Li et al., 2006) or methods using laser ablation (Tsuhi et al., 2002). Among these methods micro emulsion method is one of the versatile preparation technique which enables control of particle properties such as size, geometry, morphology, homogeneity and surface area (Hu et al., 2009; Pileni, 2003). Many reviews have been written which discuss different aspects of microemulsions (Pileni,2001, 2007, 2008; Lopez-Quintela et al., 2004; Cushing et al., 2004; Shervani et al., 2006; Holmes et al., 2003). The microemulsion method has been used to synthesize colloidal metals, colloidal Fe_3O_4, colloidal AgCl, nanocrystalline Fe_2O_3, TiO_2, Al_2O_3, and high-Tc oxide $YBa_2Cu_3O_7$ (Boutonnet et al., 1982a,b;

Bandow et al., 1987; Ayyup et al., 1988; Hou and Shah, 1988; Lal et al., 1998; Zhang et al., 2002). This review aims to give a vivid look on the use of microemulsions for synthesizing and controlling the grain size and morphology of the nanoparticles and at the same time will summarize the most recent work carried out in the synthesis of organic and inorganic nanoparticles by this method.

2. Microemulsions: past and current state

The word microemulsion was originally proposed by Schulman et al. (1959). They prepared a quaternary solution of water, benzene, hexanol, and *k*-oleate which was stable, homogenous and slightly opalescent. These systems became clear as soon as a short chain alcohol was added. In the years between 1943 and 1965 Schulman and co-workers described how to prepare these transparent systems. Basically a coarse (or macro) emulsion was prepared and the system was then titrated to clarify by adding a co-surfactant (second surface active substance). When the combination of the four components was right, the system cleared spontaneously. Most of the work reported by Schulman dealt with four component systems. Hydrocarbons (aliphatic or aromatic), ionic surfactants, co-surfactants (generally 4–8 carbon chain aliphatic alcohol) and an aqueous phase. Schulman had previously published extensively in the field of monolayers and applied what he had learnt in that field to explain the formation of microemulsions. He proposed that the surfactant and co-surfactant, when properly selected, form a mixed film at the oil/water interface, resulting in an interfacial pressure exceeding the initial positive interfacial tension. To summarize, the basic observation made by Schulman and co-workers was that when a co-surfactant is titrated into a coarse microemulsion composed of a mixture of water/surfactant in a sufficient quantity to obtain microdroplet, the result may be a system which is low in viscosity, transparent, isotropic, and very stable. The titration from opaque emulsion to transparent solution is spontaneous and well defined. It was found that these systems are made of spherical micro droplets with a diameter between 600 and 8000 nm. It was only in 1959 that Schulman proposed to call these systems microemulsions. Previously he used terms such as transparent water and oil dispersion, oleophatic hydromicelles or hydropathic oleomicelles. Since this time, microemulsions have found a wide range of applications, from oil recovery to synthesis of nanoparticles, as reported by Chhabra et al. (1997). Microemulsions are isotropic, macroscopically homogeneous, and thermodynamically stable solutions containing at least three components, namely a polar phase (usually water), a nonpolar phase (usually oil) and a surfactant. On a microscopic level the surfactant molecules form an interfacial film separating the polar and the non-polar domains. This interfacial layer forms different microstructures ranging from droplets of oil dispersed in a continuous water phase (O/W-microemulsion) over a bicontinuous "sponge" phase to water droplets dispersed in a continuous oil phase (W/O-microemulsion). The latter can be used as nanoreactors for the synthesis of nanoparticles with a low polydispersity (Julian et al., 2006; Destree et al., 2008; Zhong-min et al., 2007; Wanzhong et al., 2006). Different types of microemulsions are known, such as water-in-oil (W/O), oil-in-water (O/W) and water-in-sc-CO_2 (w/sc-CO_2).

3. Reverse micelles as nanoreactor

Surfactant molecules are dissolved in organic solvents to form spheroidal aggregates that are called as reverse micelles (Pileni, 1989). Here the polar head groups point inwards towards the core. Reverse micelles can be formed in the presence or absence of water. If the medium is free of water then aggregates are very small, while the presence of water makes large surfactant aggregates. Water is readily solubilized in the polar core and form "water pool" contents. These water pool contents are characterized by W i.e. water-surfactant molar ratio. The aggregates containing a small amount of water ($W^\circ < 15$) are usually called reverse micelles whereas aggregates corresponding to droplets containing a large amount of water molecules ($W^\circ > 15$) are called microemulsions (Luisi et al., 1986). Depending on the proportion of various components and the hydrophilic-lipophilic balance value of the surfactant used, the formation of microdroplets can be in the form of oil-swollen micelles dispersed in water as oil-in-water (O/W) microemulsion or water swollen micelles dispersed in oil as for water–in-oil (W/O) microemulsion, also called reverse microemulsion (Fig. 1). These nanodroplets can be used as nanoreactors to carry out the chemical reactions (Fig. 1). It was initially assumed that these nanodroplets could be used as templates to control the final size of the particles, however, the research carried out in the last few years has shown that besides the droplet size, several other parameters also play an important role in the final size distribution.

In short, reverse micelles can be defined as "Water in oil microemulsion in which polar head groups of surfactant molecules are attracted by aqueous core and directed towards inside and hydrocarbon chain i.e. a polar part is attracted by non aqueous phase and directed towards outside". It consists of nanometer sized, monodispersed water droplets. It can easily control the size and shape of the aqueous core by varying the value of W°. The reverse-micelles obtained at a particular ratio of the aqueous phase to the surfactant leads to uniform-size nanoreactors and have an aqueous core of 5–10 nm (Luisi et al., 1986) in which it is possible to precipitate the inorganic and organic material.

Apart from the use of reverse micelles in synthetic chemistry, it can also be used in synthesis of biologically important systems, e.g. reactions based on enzymes are basically performed in aqueous solution. The conversion of non-polar

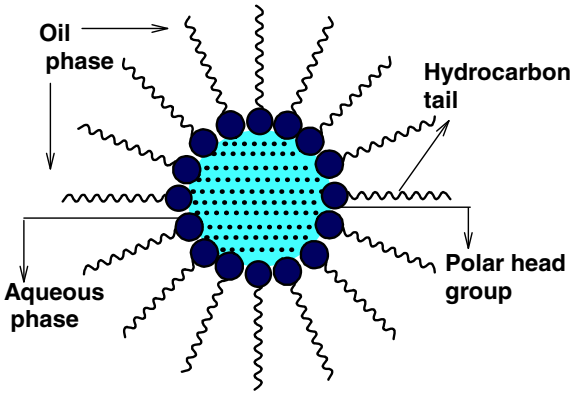

Figure 1 A typical structure of reverse micelle.

substrates is impossible. The use of reverse micelles allows one to convert either water or oil – soluble substrates into products. During the water pool exchange, non-polar compounds are in contact with the enzyme favoring the catalytic reaction (Fletcher et al., 1986).

4. Water-in-oil (W/O) micro emulsions

A "water-in-oil" micro emulsion is formed when water is dispersed in a hydrocarbon based continuous phase, and is normally located towards the oil apex of a water/oil/surfactant triangular phase diagram. In this region, thermodynamically driven surfactant self-assembly generates aggregates known as reverse or inverted micelles (Ekwall et al., 1970); spherical reverse micelles, which minimize surface energy, are the most common form. Added polar or ionic components will become compartmentalized into the central cores of these reversed micelles, hence affording fine dispersion of inorganic and organic materials in oil (Fig. 2). It is important to recognize that these systems are dynamic i.e. micelles frequently collide via random Brownian motion and coalesce to form dimers, which may exchange contents then break apart again. Clearly, any inorganic reagents encapsulated inside the micelles will become mixed. This exchange process is fundamental to nanoparticle synthesis inside reversed micellar 'templates', allowing different reactants solubilized in separate micellar solutions to react upon mixing. Micelles in these systems can be described as "nanoreactors", providing a suitable environment for controlled nucleation and growth. In addition, at the latter stages of growth, steric stabilization provided by the surfactant layer prevents the nanoparticles from aggregating (Lopez-Quintela et al., 2004). In general there are two methods for nanoparticle synthesis using microemulsion techniques (Osseo-Asare and Arriagada, 1990). The first method is called the one microemulsion method. This method includes "energy triggering" and the "one micro emulsion plus reactant" method. In the energy triggering method, the reaction is initiated by implementing a triggering agent into the single micro emulsion which contains a reactant precursor (Fig. 3a). This fluid system is activated in order to initiate the reactions that eventually lead to particle formation. For example, pulse radiolysis and laser photolysis have been used to trigger the preparation of nanosize gold particles (Kurihara et al., 1983). However in one microemulsion plus reactant method, the reaction is initiated by directly adding the pure reactant (liquid or gaseous phase) into the micro emulsion containing another reactant (Fig. 3b). The ions e.g. metals are first dissolved in the aqueous phase of a W/O microemulsion. Then the precipitating agent, in the form of an aqueous solution e.g. salt NaOH or a gas phase e.g. NH_3 (g), $CaCO_3$ (g), is fed into the micro emulsion solution. Another scenario within the one micro emulsion-plus reactant method is that the precipitating agent is first dissolved in the polar core and a metal-containing solution (e.g. organic precursor) is subsequently added into the micro emulsions. The one-micro emulsion method generally is driven by the diffusion-based process, since the second trigger/reactant is diffusing into the droplets containing the reactant in the used micro emulsion. The second method which is also often used for preparing nanoparticles is the two micro emulsion methods. Two reactants A and B, which are dissolved in the aqueous nanodroplets of two separate micro emulsions are mixed as shown in (Fig. 4). This method relies on fusion-fission events between the nanodroplets.

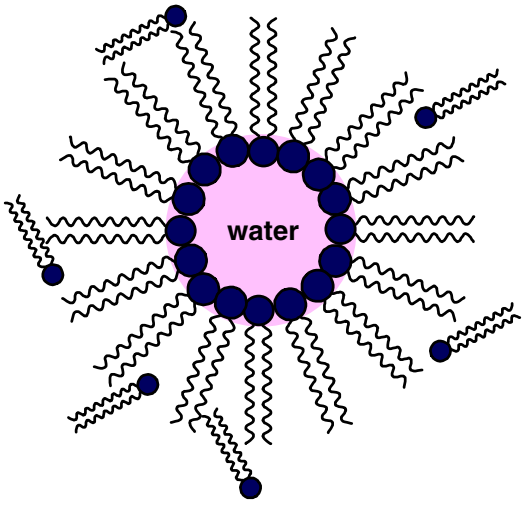

Figure 2 Water in oil microemulsion.

In order to produce the nanoparticles, two micro emulsions carrying the appropriate reactants are mixed. The Brownian motion of the micelles leads to intermicellar collisions and sufficiently energetic collisions lead to a mixing of micellar contents. The chemical reaction starts when there are fusion-fission event between the droplets as a perquisite for the mixing of the reactants. After the chemical reaction has taken place at the nanodroplets, critical number of molecules is produced (N_{crit}), this results in nuclei formation and furthermore leads to the growth of nanoparticles.

The micelles undergo numerous collisions and thereby the reactants are exchanged, mixed, and react to form the product. Nanoparticles of different materials have been prepared using this technique. The particles produced by the simple addition method can be much larger than the original droplet size but in the latter method the sizes are much smaller than the original droplet size (Li and Park, 1999). In the micro emulsions mixing method, the two reactants are pre micellized in two separate micro emulsions and are brought into contact through intermicellar exchange to conduct the reaction. In some cases, where reaction rates are very rapid, the overall reaction rate is governed by the intermicellar exchange rate. Unlike in gas-liquid systems, here the fusion-fission and exchange of contents between colliding micelles lead to reaction and also disrupt the initially established Poisson distribution of the reactant in the micelles. The intermicellar exchange rate plays a significant role in the nanoparticle formation and the effect has been studied (Bagwe and Khilar, 2000). Different research groups have obtained trends for the effect of intermicellar exchange rate (Bagwe and Khilar, 2000), water-to-surfactant molar ratio (Monnoyer et al., 1995), and concentration of reactants (Monnoyer et al., 1995). Some differences exist in the literature on the effect of these parameters on the terminal particle sizes. For instance, different research groups have reported qualitatively different findings on the effect of water-to-surfactant molar ratio on the terminal particle size (Monnoyer et al., 1995; Bagwe and Khilar, 2000). Although the formation process involves diffusion, collision, exchange, reaction, nucleation, and growth of nuclei, timescale analysis of these processes leads to different models. One of the early attempts

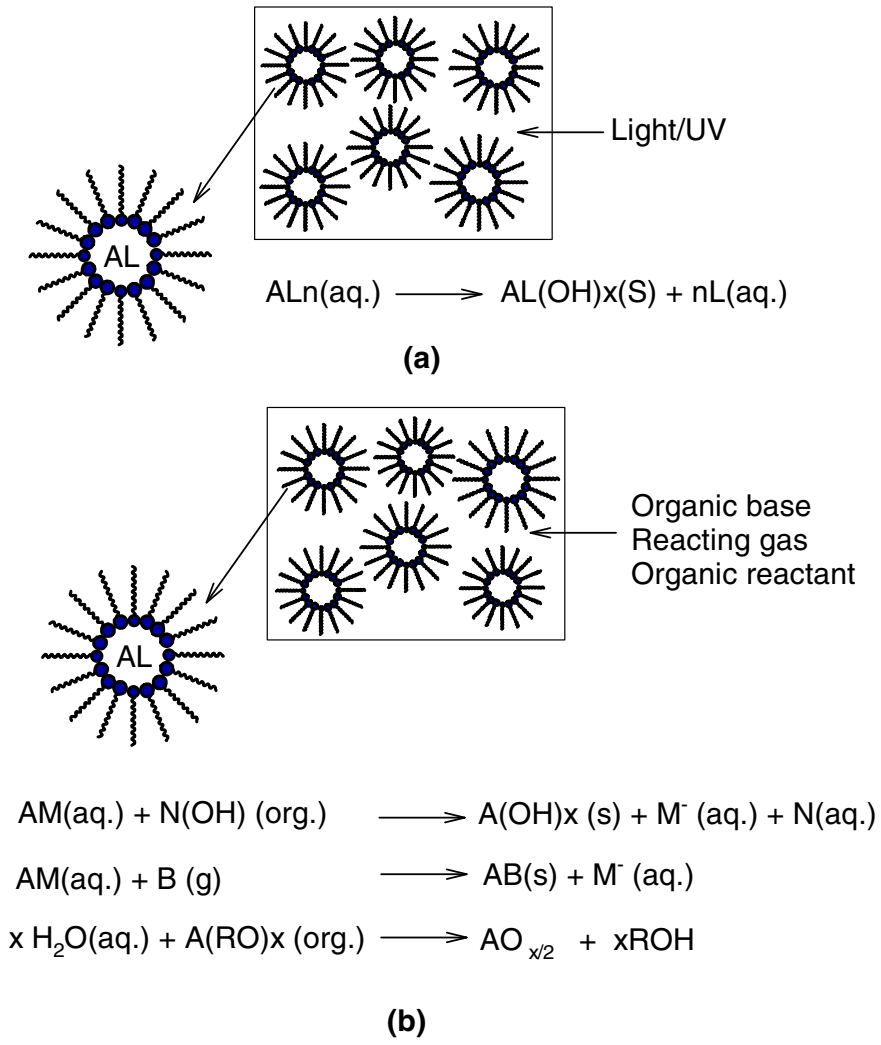

Figure 3 Different methods of nanoparticle synthesis in micro emulsions: (a) one microemulsion method: energy triggering method and (b) one-micro emulsion method plus reactant method.

was by Nagy (1989), who provided a very simplified analysis of precipitation process in the case of the single-micro emulsion method, by assuming that all the reaction and nucleation are completed initially and the remaining non nucleated micelles contribute to the growth of the already formed nuclei. Natarajan et al. (1996) extended this model by considering fusion-fission mechanisms for the intermicellar exchange process, which leads to nuclei formation in micelles having atoms greater than the critical nucleation number and also subsequent growth of the nucleus. Reaction, nucleation, and growth were assumed to be instantaneous processes. Bandyopadhyaya et al. (1997) developed a model to describe the formation of $CaCO_3$ nanoparticles considering finite rates for nucleation and diffusion of gas into a micelle.

5. Oil-in-water (O/W) microemulsions

The increasing interest regarding microemulsion systems arises essentially from their numerous potential applications in various branches of modern science or technology. Microemulsions can be prepared in a narrow temperature range (usually 10–20 °C). One of the ways to overcome this problem is to use a mixture of ionic and non-ionic surfactants, as ionic surfactants are effective with a wide range of temperature whereas non-ionic surfactants exhibit large solubilizing power. By using a proper mixture of ionic and non-ionic surfactants one could increase the temperature range for producing O/W microemulsions. By increasing the pH of the microemulsion more carboxylic acid groups are neutralized and the negative charge at the interface provides the double layer which enhances the formation of O/W microemulsion. The charged head group of the microemulsion droplets is the driving force for producing O/W microemulsion with a wide range of temperatures. Normal micelles can solubilize more oil in the hydrocarbon core, forming swollen micelles which are oil-in-water (O/W) microemulsions. Varying the concentration of the dispersed phase and the surfactant it is possible to tailor the size of the droplets in the range 1–100 nm, approximately. The use of an aqueous continuous phase allows for the incorporation of the organic droplets (micelles) and thereby decreasing the use and the human exposure to organic solvents. Moreover, the micelles (oil-in-water) (Fig. 5) can also be used as carriers or containers of a wide number of organic compounds or particles, e.g. optical limiting units. The

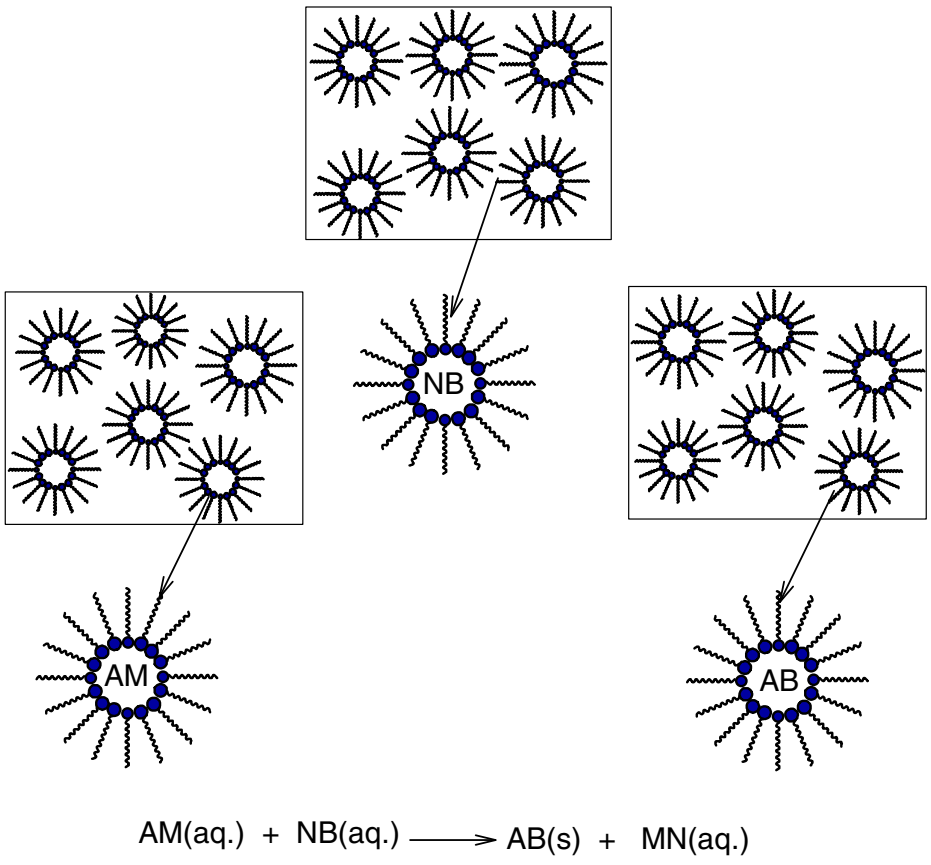

Figure 4 Two-microemulsion method. Cations: A, N, Anions: B, M.

reversed micelles (water-in-oil) can also be used to carry inorganic compounds. The O/W microemulsions were prepared following the phase diagram reported by Wang et al. (1995). The compositions were calculated from the phase diagram and exact amounts of surfactant and co-surfactant were dissolved in water. A small volume of heptane was then added, stirred mechanically, and sonicated for 5 min in an ultrasonic bath to form the oil-in water microemulsion. Different microemulsions were prepared by varying the concentration of surfactant and dispersed phase, which gave micelles with different droplet size. The droplets constituting the dispersed phase of an oil-in-water microemulsion can be used as carriers of lipophilic solutes across an aqueous environment.

6. Bicontinuous microemulsions

The bicontinuous structure or sponge phase is a quite intricate structure. As its name suggests, in this structure water and oil are continuous phases. The sponge structure is a good example: the sponge has a continuous structure, but it is possible to "fill" the sponge with a liquid. The liquid forms a continuous phase and the material of sponge also forms a continuous phase. Thinking that the sponge surface is the surfactant, we present a cartoon of a bicontinuous structure below: bicontinuous structures are perhaps more frequently observed than discrete micellar aggregates. They are encountered in microemulsions, in mesophases, and even in relatively dilute surfactant solutions. Furthermore, structures that cannot be described in terms of particles and also ubiquitous in nanophilic systems: zeolites, copolymer molecular metals, volcanic minerals, surfactant-templated synthetic mesoporous oxides (Anderson et al., 2006), and composite media. As first proposed by Scriven (Fig. 6a), there are no longer isolated droplets but rather a bicontinous arrangement of oil and water channels. Most of the microemulsions that are bicontinous contain comparable amounts of water and oil, and most interesting are those that are stabilized by only small amount of surfactants (Kresge et al., 1992). The first experimental demonstration that microemulsions may indeed be bicontinuous came from NMR self-diffusion studies (Lindman and Oisson, 1996). The relatively high diffusion coefficient of both water and oil suggests that some continuity must exist between the water and the oil domains. The demonstration of a microemulsion with a mean curvature on the average of zero is a strong indication of bicontinuity. A further possible bicontinuous microstructure, considered in relation to water-poor system, is similar to a hexagonal liquid crystal structure, where one of the liquid lies inside interconnected tubules or conduits. The model structures that were proposed for the description of bicontinuous system satisfy the mathematical constraint that the dividing surface between hydrophilic and hydrophobic domains is a surface of constant mean curvature. In microemulsions the structure is lacking any long-range order and the mean curvature over the dividing surface is not homogenous at any given instant. However, we can visualize bicontinuous microemulsion structure using well-defined models (continuous paths between interconnected spheres, distorted lamellae, tubule structures with one of the solvents confined

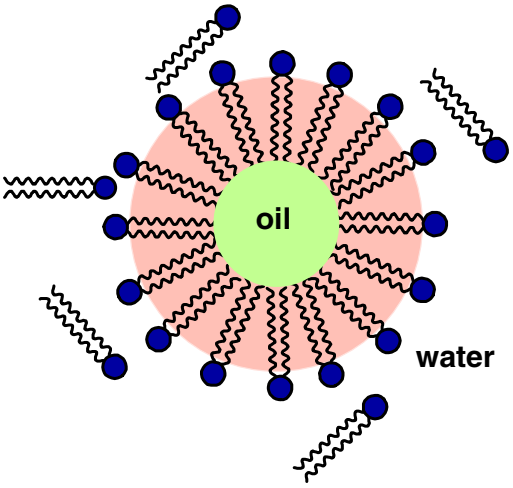

Figure 5 Oil in water microemulsion.

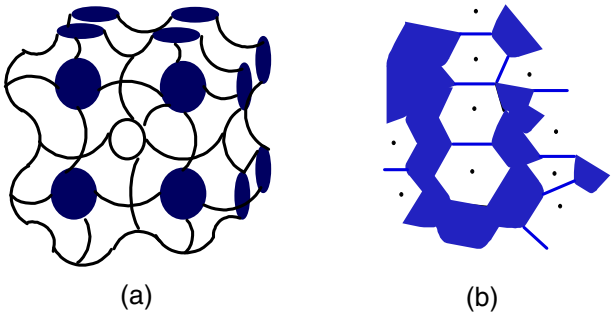

Figure 6 Bicontinuous structure.

to branched tubes, and a minimal surface type of structure similar to that established for bicontinuous cubic phase) but picture them as being thermally disrupted or melted. Talmon and Prager were the first to provide a thermodynamic model for bicontinuous microemulsion (Fig. 6b).

7. Supercritical CO_2 microemulsions

Much attention has been paid to the synthesis of nanoparticles in water-in-supercritical CO_2 microemulsions (Ohde et al., 2001, 2002a,b,c). Using conventional water-in-oil microemulsions for nanoparticle synthesis, the main problem which arises is the separation and removal of solvent from products. Supercritical carbon dioxide used as a solvent offers several advantages such as fast reaction speed, rapid separation and easy removal of solvent from nanoparticles. This method has been used to produce Ag and Cu (Ohde et al., 2001) and CdS and ZnS (Ohde et al., 2002) nanoparticles. Hydrogenation of olefins catalysed by Pd nanoparticles in a water-in-CO_2 microemulsion has also been reported by Ohde et al. (2002a,b,c).

The selectivity coefficients for the counterion exchange in the water-AOT-heptane microemulsion interface were determined by using pseudo-phase ion exchange formalism (Goncalves et al., 2003). Theoretical results have been successfully compared to quenching of the RuL_3^{4-} luminescence emission measurements. Finally, the catalytic activity of metallic particles synthesized in AOT microemulsions has been a field of high activity. Using water/AOT/supercritical CO_2 microemulsions, Ohde et al. (2002a,b,c) showed that hydrogen gas can cause reduction of a number of metal ions including Pd^{2+} dissolved in the water core of the microemulsion. After reduction, the hydrogen gas can also serve as a starting material for in situ hydrogenation in supercritical CO_2. The hydrogenation of 4-methoxycinnamic acid to 4 methoxyhydrocinnamic acid, hydrogenation of trans-stilbene to 1,2-diphenylethane and hydrogenation of maleic acid to succinic acid were performed in supercritical CO_2 microemulsions catalysed by Pd nanoparticles (size range of about 5–10 nm). Further studies (Ohde et al., 2002a,b,c) have shown that rhodium nanoparticles dispersed in CO_2 microemulsions are also effective catalysts for rapid hydrogenation of arenes in supercritical CO_2.

8. Mechanism and dynamic of nanoparticle synthesis

The aqueous droplets continuously collide, coalesce, and break apart, resulting in a continuous exchange of solution content. In fact, the half-life of the exchange reaction between the droplets is of the order of 10^{-3}–10^{-2} s (Atik and Thomas, 1981a). Two models have been proposed to explain the variation of the size of the particles with the precursor concentration and with the size of the aqueous droplets. The first is based on the LaMer diagram (La Mer and Dinegam, 1950), which has been proposed to explain the precipitation in an aqueous medium and thus is not specific to the micro emulsion. This diagram (Fig. 7) illustrates the variation of the concentration with time during a precipitation reaction and is based on the principle that the nucleation is the limiting step in the precipitation reaction. In the first step the concentration increases continuously with increasing time. As the concentration reaches the critical supersaturation value, nucleation occurs. This leads to a decrease of the concentration. Between the concentrations C^*_{max} and C^*_{min} the nucleation occurs. Later the decrease of the concentration is due to the growth of the particles by diffusion. This growth occurs until the concentration reaches the solubility value. This model has been applied to the micro emulsion medium, i.e., that nucleation occurs in the first part of the reaction and later only growth of the particles occurs. If this model is followed, the size of the particles will increase continuously with the concentration of the precursor or a minimum in the variation of the size with the concentration can also be expected. This stems from the fact that the number of nuclei is constant and the increase of

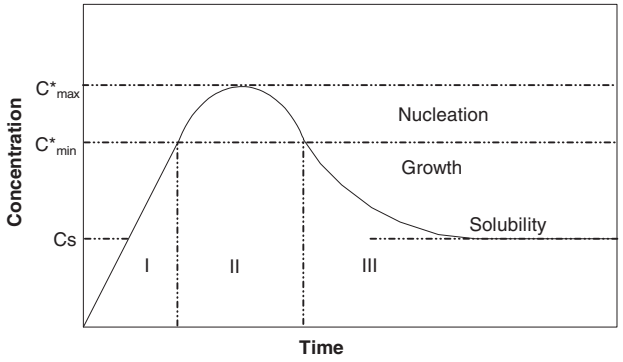

Figure 7 LaMer diagram.

concentration leads to an increase of the size of the particles. The second model is based on the thermodynamic stabilization of the particles (La Mer and Dinegam, 1950). In this model the particles are thermodynamically stabilized by the surfactant. The size of the particles stays constant when the precursor concentration and the size of the aqueous droplets vary. The nucleation occurs continuously during the nanoparticle formation. These two models are limiting models: the LaMer diagram does not take into account the stabilization of the particles by the surfactant, and the thermodynamic stabilization model does not take into account that the nucleation of the particles is more difficult than the growth by diffusion.

Because the process of nanoparticles formation is stochastic in nature, Monte Carlo simulation is probably a natural choice to explain the mechanism of formation of microemulsions; however, it is computationally intensive given that the number of micelles to be considered in a simulation can be very large. A mean field approximation with Monte Carlo simulation is probably needed to account for all the possible combinations of various species in the micelles and outcomes of the fusion-fission events. The population balance equations with mean field approximation, restricting the maximum number of molecules in a micelle, can be solved and the particle size distribution (PSD) can be computed from the fraction of nucleated micelles. The different stages of nanoparticle formation process inside water droplets can be explained as: chemical reaction, nucleation and particle growth. Two different reactants (A and B) are introduced in these microemulsions. For metal oxalate, A should be a metal ion and B should be the oxalate ion. These two microemulsions are mixed up by constant stirring and the droplets continuously collide, which results in the interchange of reactants. During this process, the reaction takes place inside the nanoreactor. The different steps are shown schematically in Fig. 9. The mechanistic steps for the formation of nanoparticles may be explained by Fig. 10.

8.1. Chemical reactions

The very first step of nanoparticle formation in microemulsion system is the chemical reaction between the two reactants trapped in microemulsion cores, or the reaction between the reactant and the precipitating agent. Rauscher et al. (2005) presented a time scale analysis for the precipitation of $CaCO_3$ in a typical microemulsion system, where typical time constants for the chemical reaction τ_{chem} (10^{-12}–10^{-8}), the droplet exchange τ_{ex} (10^{-8}–10^{-3}), and nucleation τ_{nuc} (10^{-12}–10^{-8}), and particle growth τ_g (10^{-3}–10^{-1}) were estimated. The presented time constants show that the chemical reaction and the nucleation are the fastest phenomena occurring in the microemulsion system. Due to the same time scales of these processes the chemical reaction is regarded as an instantaneous step in this study. Thus the fastest dynamics in this process is represented by the nucleation. By this implementation of the chemical reaction the product molecules C are instantaneously formed, when droplets with either one of the reactants are mixed by the droplet exchange. Thus the liquid molecules and the consequent solid precipitation molecules are formed by the following reaction scheme:

$$A + B \rightarrow C \downarrow + D$$

Atik and Thomas showed by their experimentally obtained data that the distribution of the dissolved salts inside the water droplets of microemulsion system followed a Poisson distribution (Atik and Thomas, 1981a). The use of a Poisson distribution in the presented model leads to the assumption that the molecules C inside all droplets of the reactor are distributed according to the Poisson distribution and that newly formed C inside one droplet is immediately distributed by the droplet exchange within the reactor to conserve this equilibrium distribution (Bandyopadhyaya et al., 2000). The Poisson distribution gives the number of droplets containing i molecules of C as Proportion pi of the total amount of droplets in the system (i is an integer number). The only parameter needed to calculate pi is the average droplet occupancy λ with liquid molecules C.

The Poisson distribution is then defined by:

$$P_i(t) = \frac{\lambda(t)^i \cdot \mathrm{Exp}^{(-\lambda(t))}}{i!} \tag{1}$$

The average droplet occupancy λ with the liquid molecules C at a specific time t is given by:

$$\lambda(t) = \frac{N_c(t)}{N_{drop}(t)} \tag{2}$$

where $N_c(t)$ is the total amount of molecules C inside the reactor in moles and $N_{drop}(t)$ is the total number of droplets inside the reactor at a specific time in moles. $N_{drop}(t)$ can be calculated from the total amount of water at a specific time $V_w(t)$ and the droplet diameter d_{drop}. This relation is given by

$$N_{drop}(t) = \frac{V_w(t)}{K_{vd} \cdot d_{drop}^3 \cdot N_A} \tag{3}$$

where k_{vd} is the droplet shape factor and N_A is Avogadro's number.

8.2. Nucleation

In a highly supersaturated solution the instability of the system will result in a fast local concentration fluctuation. This leads in a homogeneous phase to small solid clusters of molecules. These clusters are assumed to be formed by the mechanism of addition of dissolved molecules to the cluster until a critical cluster size is reached. Thereby, a stable nucleus is formed (Myerson, 1983). If the cluster cannot reach the critical size, it will redissolve. In the absence of foreign particles this mechanism is considered as primary homogeneous nucleation. For primary heterogeneous nucleation, nuclei are formed on the surface of foreign solid particles. These foreign particles are generally known to reduce the surface energy being required for nucleation as there are interactions between the foreign particles, molecules, and the solvent (Hirai et al., 1993) The surface energy σ can drop from around 0.08–0.1 J/m^2 (for homogeneous nucleation) to much lower values of about 0.002–0.003 J/m^2 (for heterogeneous nucleation). Fig. 8 illustrates that homogeneous nucleation occurs at very high supersaturation and heterogeneous nucleation occurs at much lower supersaturation. After the establishment of the Poisson distribution of the molecules C, the second step of the nanoparticle formation i.e., nucleation occurs inside the water droplets similar to the known bulk phase precipitation reaction scheme. New particles P are born if the number of C molecules inside one droplet is greater than the critical number of molecules needed to form a stable nucleus N_{crit} (Alejandra and Reinhard, 2006; Voigt et al., 2005).

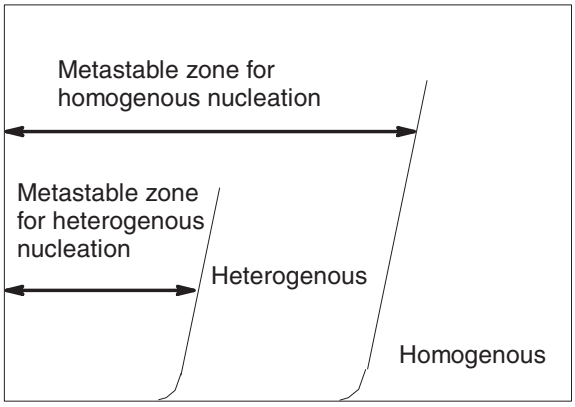

Figure 8 Scheme of the dependencies of the primary nucleation rate B on the supersaturation ratios.

The nucleation mechanism can be represented by the following scheme:

$$N_{\text{crit}}C \rightarrow P$$

The molecular nucleation rate r_{nuc} of the dissolved C can be obtained from the nucleation rate B_{nuc} and Avogadro's number N_{A} according to equation

$$r_{\text{nuc}} = \frac{B_{\text{nuc}}}{N_{\text{A}}} \tag{4}$$

8.3. Growth

The growth of the small nuclei to bigger particles can be initiated by several mechanisms. Mechanisms like transport of dissolved reactant (e.g. $BaSO_4$) molecules by diffusion or by convection to the particle surface followed by a reaction on the surface or the agglomeration of small nuclei can be responsible for particle growth. In the case of microemulsion precipitation, the second mechanism can be neglected due to the protecting surfactant monolayer around each droplet and the very low occupancy of droplets with particles (Alejandra and Reinhard, 2006). The growth of one particle P into a bigger particle P' by the consumption of C is expressed by equation:

$$P + C \rightarrow P'$$

The consumption rate of dissolved molecules C due to growth can be represented by r_g and is derived from the total molar transfer flux due to crystal growth (Jain and Mehra, 2004) by:

$$r_{\text{g}} = \frac{3 \cdot K_{\text{vp}} \cdot \rho_{\text{C}}}{M_{\text{C}}} \int_0^{\infty} d_p^2 \cdot G.f(d_{\text{p}}) \cdot d(d_{\text{p}}) \tag{5}$$

where k_{vp} is the particle shape factor, ρ_{C} and M_{C} are the density and the molecular weight of reactant molecules, respectively. The growth rate G can be interpreted as the velocity of particle growth. The integral term in the above equation is simplified by using the mean particle diameter d_{pm} instead of the whole distribution. Thereby, the particle number density function $f(d_{\text{p}})$ is replaced by the dirac delta function δ. The above equation on simplification by bringing the above mentioned changes is simplified to the following final equation:

$$r_{\text{g}} = \frac{3 \cdot K_{\text{vp}} \cdot \rho_{\text{C}} \cdot n_{\text{p}} \cdot N_{\text{A}} \cdot d_{\text{pm}}^2 \cdot G}{M_{\text{C}}} \tag{6}$$

where $N_{\text{p}} = n_{\text{p}} \cdot N_{\text{A}}$.

Similar to the nucleation rate approach, the growth rate G also depends on the concentration of the dissolved C molecules in the liquid phase.

8.4. Fusion–fission rules

The overall process of nanoparticle synthesis in microemulsion is guided by certain rules:

- The collision between two non nucleated (nonempty) micelles results in transfer of entire solute in one micelle and the formation of an empty micelle.
- The fusion between two micelles containing different reactants in each results in complete mixing of the solutes followed by reaction in one micelle and the formation of an empty micelle.
- The fusion between a nucleated and a non nucleated (nonempty) micelle results in transfer of entire solute into the micelle containing a nucleus, leading to growth of the existing nucleus and the formation of an empty micelle.

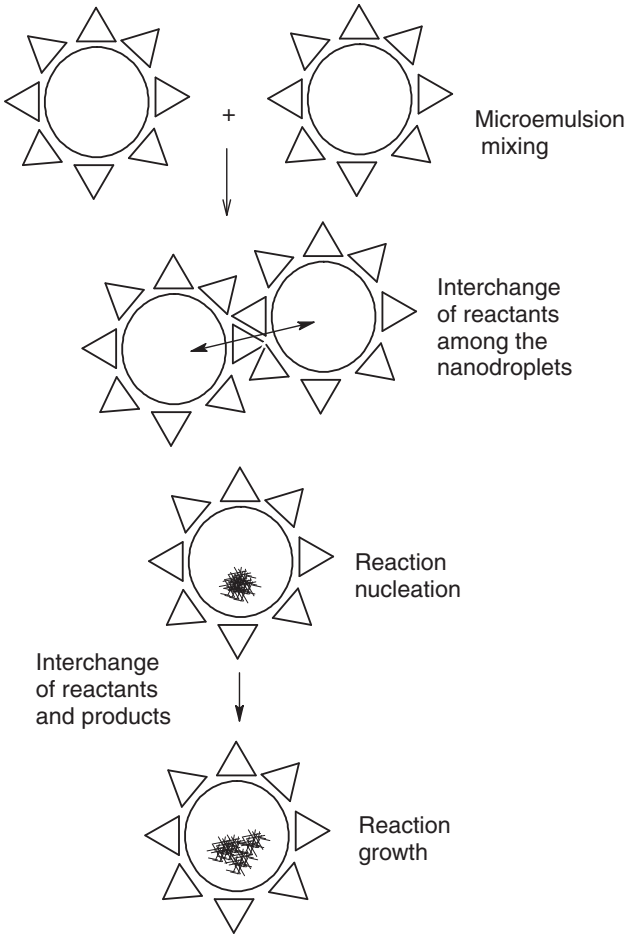

Figure 9 Mechanism of the formation of nanoparticles in microemulsions.

- The collision of any micelle with an empty micelle results in no change.
- The autocatalysis effect has been considered for collisions involving nucleated micelles.

8.5. Microemulsion dynamics

By microemulsion dynamics, we mean the fact that the domains are not static ones, but are in continuous movement and collision with each other. In each collision, material interchange can takes place. The whole process of motion-collision exchange can be characterized through a parameter τ_{ex}, which is characteristic of each kind of microemulsion. Understanding how the chemical reaction proceeds depends on the ratio between the characteristic chemical reaction time τ_r and τ_{ex}. When the reaction is very slow in comparison to the microemulsion dynamics $\tau_r/\tau_{ex} \gg 1$, the reaction sees the microemulsion as a static object, and a pseudo-phase model can be applied. In contrast, for chemical reactions with $\tau_r/\tau_{ex} <$ or $= 1$, the dynamics of the microemulsion has to be taken into account to explain the chemical reaction. If one assumes that microemulsion domains are formed by spherical droplets, the characteristic droplet's collision time in microemulsions can be easily calculated assuming that the droplets diffuse through a continuous medium with viscosity (η). Then, the collision rate constant is given by $kD = (8/3)\ k_B T/\eta \approx 10^{-9}$ M $^{-1}$ s^{-1} for a typical low viscosity solvent. Because usually the droplet's volume fraction $\Phi \approx 0.1$, i.e., (droplet) $= 10^{-3}$ M for a typical droplet's size ≈ 10 nm, the encounter rate constant $K_{enc} \approx 10^6$ s^{-1}. Thus the average collision time (encounter time) T_{enc} is ≈ 1 μs. It is well known that not all droplet collisions are effective for material exchange. This can be taken into account introducing an encounter rate factor (γ), which for a particular material (reactant) depends on the film flexibility (Kumar et al., 2004), i.e. $k_{ex} = \gamma k_{en}$. For rigid films like AOT microemulsions $= 10^{-3}$ that is, only one in each 1000 collisions is effective for the reactants exchange (Lopez-Quintela et al., 2004). However for flexible films this value can reach up to $\gamma = 10^{-1}$ (Kumar et al., 2004). Then the microemulsion exchange characteristic time τ_{ex} is in the range $= 10\ \mu s < \tau_{ex} < 1$ ms. According to (Fig. 11) reactions with a half-life reaction time τ_r, much larger than 0.01–1 ms are assumed to occur in a "static" pseudo-phase system, in which the exchange of material does not play any role in the kinetics (region III, Fig. 11). However, for reactions with a half-life reaction time τ_r far below 0.01–1 ms, the droplet's exchange is the control factor of the kinetics (I). This occurs only for reactions that are near diffusion controlled. The interplay of droplet's exchange and chemical reaction has to be taken into account for reactions with τ_r near τ_{exc} (II). Therefore, to understand chemical reactions in microemulsions, there is a need to know which model is most suitable for a particular reaction. However there are not many available data for this classification, and any study in this direction will be of valuable importance. Because film flexibility is mainly determined by the surfactant, it is convenient to classify reactions located in regions I and II

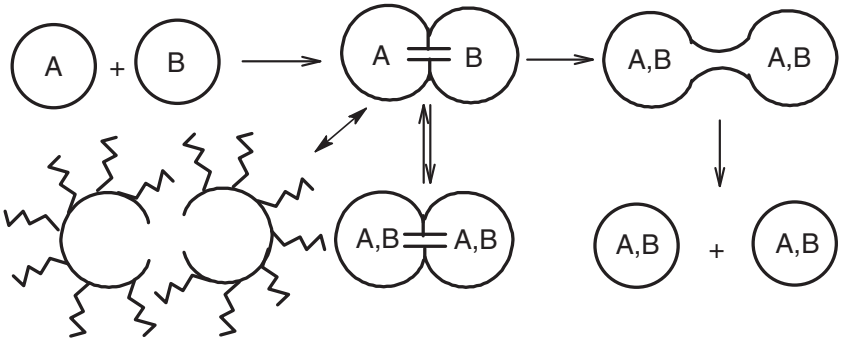

Figure 10 Mechanism for the formation of equal number of droplets.

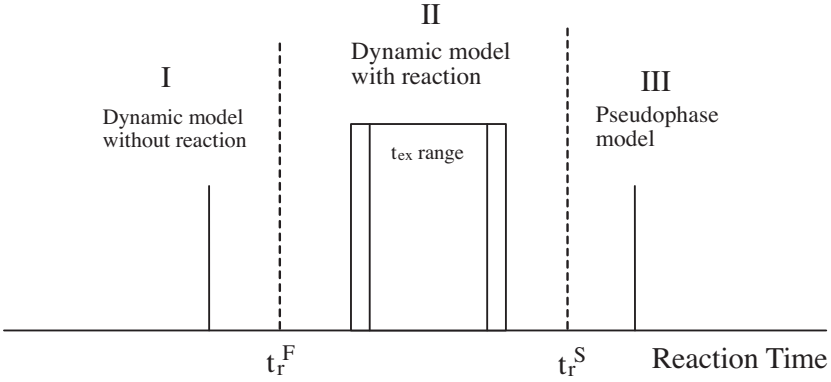

Figure 11 Reaction time τ_r versus microemulsion dynamics (τ_r).

based on the surfactants being used. This will restrict the τ_r values, corresponding to each surfactant, to a small range that, in turn, depends on other variables (such as co surfactant, oil, droplet's size) and the specific reactant to be exchanged. A more direct comparison of the different experimental results can then be achieved.

9. Phase diagrams for microemulsions

One peculiarity of microemulsions lies in the so-called 'phase inversion' that takes place at a given water-to-oil concentration ratio. At lower water content the microemulsion consists of very small water droplets dispersed in oil (W/O), while at higher water content the situation is reversed and the system consists of oil droplets dispersed in water (O/W). Between these two phases exists an intermediate situation in which the system consists of layers of surfactant separating alternate layers of water and oil. However on the w/o side more complicated structures seem to exist. By increasing the water content the droplets of water initially increase their radius slightly and then their shape undergoes a change becoming an elongated cylinder. Finally the layered status is reached from which, again increasing the water content, the system passes directly to the o/w droplets situation. The existence of this kind of structural change has been predicted on the basis of many different measurements, such as x-ray, optical properties, dielectric properties, viscosity and NMR. From the thermodynamic point of view, microemulsions are rather complicated systems, mainly because of the existence of at least four components, and because of the electric double layer surrounding the droplets, or the rods, or the layers that contribute noticeably to the free energy of the system. In addition, the actual surface tension is a variable parameter whose value is determined by the co-surfactant (alcohol) concentration of the interface. The condition of formation of microemulsions is given and the phase inversion is foreseen. However, only spherical droplets are considered. A hypothetical phase diagram of a microemulsion given by Prince (1977) is shown in Fig. 12. Because of the unusual shape of the w/o region, the alteration of the W/O droplets to a cylindrical form, along a line of fixed concentration of surfactant traverses a region in which a microemulsion cannot be thermodynamically stable. A phase may be defined as a region of component space homogeneously filled with matter. Any phase diagram is the compact graphical representation of phase boundaries of any feasible system (uni- or multicomponent). A ternary mixture of water (W), oil (O) and surfactant (S) has four independent thermodynamic variables namely pressure, temperature, and two composition variables. Out of these variables, effect of pressure is small compared to that of temperature. Assuming, that pressure is constant at atmospheric level, the phase diagram of a ternary system may then be represented in an upright prism with the Gibbs triangle as base and temperature (T) as the ordinate (Fig. 13). The composition variables are conveniently expressed in mass fraction of oil (α) in the mixture of water and oil, $\alpha = B/(A + B)$, and that for amphiphile (γ) in the mixture of all three components, $\gamma = C/(A + B + C)$, both expressed in weight percent (wt.%). Each point in the phase prism is then unambiguously expressed by a set of co-ordinate (α, γ, and T)

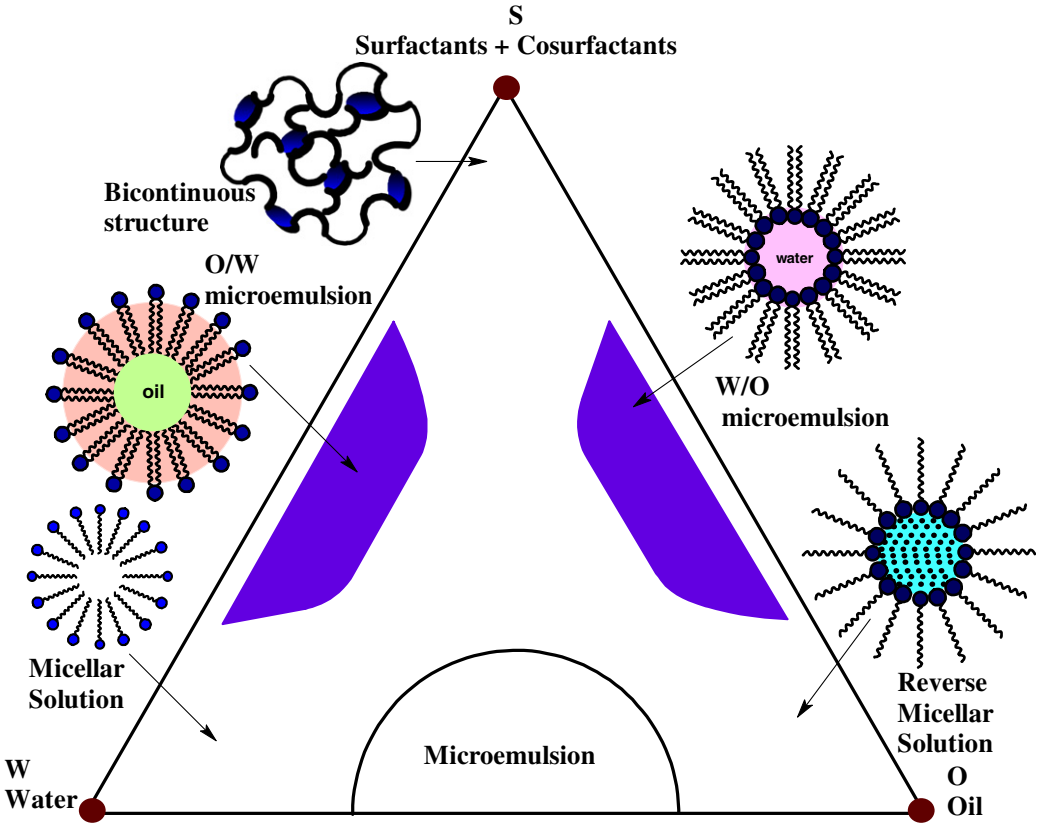

Figure 12 Hypothetical phase regions of microemulsion systems.

which represents the composition of a particular system (Fig. 13). The phase diagrams are helpful in various ways, like knowing the extent of solubilization, presence of multiphase etc., corresponding to any particular composition chosen. The microemulsion region is usually characterized by constructing ternary-phase diagrams. Three components are the basic requirements to form a microemulsion: an oil phase, an aqueous phase and a surfactant. If a cosurfactant is used, it may sometimes be represented at a fixed ratio to surfactant as a single component, and treated as a single ''pseudo-component''. The relative amounts of these three components can be represented in a ternary phase diagram. Gibbs phase diagrams can be used to show the influence of changes in the volume fractions of the different phases on the phase behavior of the system. The three components composing the system are each found at an apex of the triangle, where their corresponding volume fraction is 100%. Moving away from that corner reduces the volume fraction of that specific component and increases the volume fraction of one or both of the two other components. Each point within the triangle represents a possible composition of a mixture of the three components or pseudo-components, which may consist (ideally, according to the Gibbs' phase rule) of one, two or three phases. These points combine to form regions with boundaries between them, which represent the ''phase behavior'' of the system at constant temperature and pressure. The Gibbs phase diagram, however, is an empirical visual observation of the state of the system and may, or may not express the true number of phases within a given composition. Apparently clear single phase formulations can still consist of multiple iso-tropic phases (e.g. the apparently clear heptane/AOT/water microemulsions consist multiple phases). Since these systems can be in equilibrium with other phases, many systems, especially those with high volume fractions of both the two immiscible phases, can be easily destabilised by anything that changes this equilibrium e.g. high or low temperature or addition of surface tension modifying agents. However, examples of relatively stable microemulsions can be found. It is believed that the mechanism for removing acid build up in car engine oils involves low water phase volume, water-in-oil (W/O) microemulsions. Theoretically, transport of the aqueous acid droplets through the engine oil to microdispersed calcium carbonate particles in the oil should be most efficient when the droplets are small enough to transport a single hydrogen ion (the smaller the droplets, the greater the number of droplets, the faster the neutralisation). Such microemulsions are probably very stable across a reasonably wide range of elevated temperatures. A very convenient method for preparation of a microemulsion and construction of planer triangular phase diagram is the titration procedure. A surfactant is dissolved in an inaqueous (or organic) medium and is titrated with organic (or aqueous) phase. The transition points (turbid and transparent) are noted. The single-phased, optically transparent domains correspond to the microemulsions whereas turbid zones are for multiphase systems. Repeating the same procedure for different concentrations of surfactant solution, almost all transition points can be noted. Thus, a triangular phase diagram can easily be drawn. Any mixture of three components, *A*, *B*, and *C* can be represented using properties of an equilateral triangle (ternary diagrams, Figs. 12–14). The relative amounts of *A*, *B* and *C* are expressed in percentage of the selected parameter, such as:

$$A\% + B\% + C\% = 100\% \tag{7}$$

Only two percentages are independent, the third one can be obtained by the Eq. (7) (Fig. 13) shows how the given mixture can be plotted. Point M is obtained at the crossing of the respective percentage values of *A*, *B* and *C*. Eq. (7) cannot be used in four components microemulsions, unless a pseudo-component is defined, such as a given ratio of surfactant to alcoholic co surfactant. This active mixture is considered as a third component and is placed at the *C* apex.

The composition of the mixture is specified by the composition variables a and g, where *a* is the weight fraction of oil in the mixture of oil and water:

$$\alpha = \frac{m_{\text{Oil}}}{m_{\text{Oil}} + m_{\text{Water}}} \tag{8}$$

and *g* is the weight fraction of surfactant in the ternary mixture:

$$\gamma = \frac{m_{\text{surfactant}}}{m_{\text{Water}} + m_{\text{Oil}} + m_{\text{Surfactant}}} \tag{9}$$

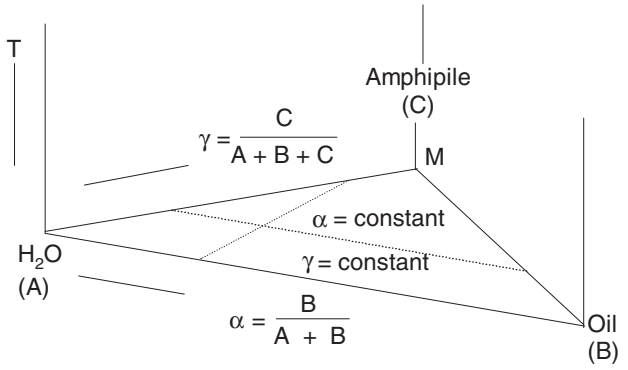

Figure 13 The ternary phase diagram representation. Point M represents the liquid composition with 59% of *A*, 9% of *B* and 32% of *C* (total 100%) The percentage can be mass, volume or mole percentages.

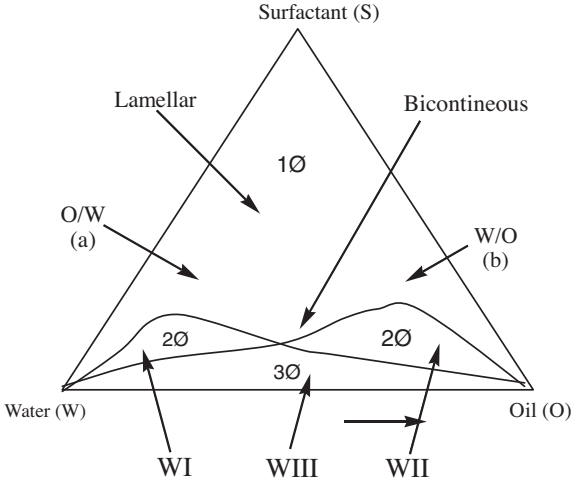

Figure 14 Phase prism with the Gibbs phase triangle as base (ABC) and the temperature axis (*T*) as ordinate.

The phase behavior of mixtures of water, *n* alkane and alkyl polyethyleneglycol ether type surfactants (C*i*E*j*) has systematically been studied in the last two decades.

10. Factors affecting microemulsion dynamics

10.1. Surfactants and co-surfactants in microemulsions

The surface active agents or surfactant molecules are amphiphilic in character, i.e., they possess hydrophilic and hydrophobic regions in their molecules. They have a long hydrocarbon tail and a relatively small ionic or polar head group. Amphiphiles can be ionic (cationic, anionic), zwitterionic, or nonionic depending on the nature of their head groups. Cetyltrimethylammonium bromide provides a very flexible film, which gives rise to a high exchange dynamic of the micelles. In recent years, an increasing number of works used CTAB as surfactant. (Porta et al., 2002) obtained smaller Au nanoparticles using CTAB as a surfactant. Chen and Wu (2000) studied the influence of reactants, metal salt and reducing agent on the final Ni nanoparticle size in a water/CTAB/*n*-hexanol microemulsion. ZrO_2–Y_2O_3 nanoparticles have been obtained in a CTAB/hexanol/water microemulsion by Fang and Yang (1999). In their report, these authors noted a peculiar behavior; nanoparticle size distribution is narrowed down in two cases, increasing the water content at fixed surfactant concentration or decreasing the surfactant content at fixed water content. Both cases led to larger droplets. This kind of microemulsions has also been used to produce other materials spinel $ZnAl_2O_4$ (Giannakas et al., 2003), perovskite $nLaMnO_3$ (Giannakas et al., 2003), bioceramic hydroxyapatite (Koumoudilis et al., 2003), cerium oxide (Wu et al., 2002), and coated materials like, SiO_2-coated Pt, Pd and Pt/Ag (Yu et al., 2003). The catalytic activity of nanoparticles synthesised in CTAB microemulsions has also been studied by Sun et al. (2001).

The anionic surfactant perfluoropolyethercarboxylic acid was converted to its ammonium salt by reaction with excess ammonium hydroxide. This surfactant has been used in water-in-carbon dioxide microemulsions (Sun et al., 2001; Stallings and Lamb, 2003) to produce Ag nanoparticles (Nagashima et al., 2003) and Ti (Sun et al., 2001). Triton X-100 has been used to prepare different kinds of nanoparticles: CeO_2, Ce1-x-$ZrxO_2$, Ce–Tb mixed oxides, Al_2O_3, Y_2O_3:$Eu3^+$, TiO_2 and silver halides (Rodriguez et al., 2003; Hungrıa et al., 2003; Pang and Bao, 2002; Pang et al., 2003; Andersson et al., 2002; Xu and Li, 2003). Zhang and Chan (2003) studied the formation of Pt–Ru bimetallic nanoparticles using a water-in-oil reverse microemulsion of water/Triton X-100/propanol/cyclohexane. Zhang and Chan (2002) also studied the synthesis of Pt–Co nanoparticles using the same microemulsion. Silica-coated iron oxide nanoparticles were studied by Santra et al. (2001) using different precipitating agents (NH_4OH or NaOH) and surfactants (Triton X, Brij 97 and Igepal). They found that the ultra small synthesized particles (< 5 nm) aggregate in different morphologies. Results are explained, assuming that the extent of surfactant adsorption on to the particle surface varies depending on the experimental conditions. The more ordered structures observed with Brij 97 are attributed to its longer hydrophobic chain (compared to Triton X and Igepal), promoting a more ordered particle aggregation, due to stronger hydrophobic–hydrophobic interactions between the oleyl groups attached to adjacent nanoparticles. The authors do not exclude the influence of the ultrasounds used during the reaction on the adsorption process. Different results were obtained by Tartaj and Serna (2002). These authors found that the nature of the surfactant (Igepal CO-720 or Triton X-100) did not significantly affect the microstructure of the prepared iron oxide nanoparticles, using cyclohexane as oil and n-hexanol as cosurfactant. Poly(oxyethylene)-5-nonylphenol ether (NP-5), poly(oxyethylene)-9-nonylphenol ether (NP-9) and poly(oxyethylene)-12-nonylphenol ether (NP-12) have been recently used to prepare different particles, such as hydroxyapatite (Bose and Saha, 2003), metallic bismuth (Fang et al., 2001), and also applied in catalytic activity studies (Liu et al., 2002). Rh nanoparticles have been synthesized in NP-5/cyclohexane microemulsion (Althues and Kaskel, 2002). At a fixed $RhCl_3$ and surfactant concentration, and fixed W value, ultrafine Rh particles were obtained using different reducing agents (H_2, $NaBH_4$ and N_2H_4). Different final particle sizes were obtained, depending on the reactants nature. Pt–Ru bimetallic nanoparticles have been prepared by using these nonionic surfactants (Liu et al., 2002). Silica-coated Rh nanoparticles were also reported (Althues and Kaskel, 2002).

Brij 30, a nonionic surfactant was used to study the immobilization of ZnS nanoparticles synthesised in microemulsions to silica (Althues and Kaskel, 2002), and to prepare silica coated iron oxide (Santra et al., 2001). In a very interesting paper, various surfactants have been compared for the synthesis of silica coated zinc ferrite nanoparticles (Hanaoka et al., 2001). Pentaoxyethylene-glycol-nonyl-phenyl ether, commonly known by Igepal-CO520, is a nonionic surfactant which was used by Bae et al. (2002) to study the influence of [water]/[TEOS] molar ratio on the final size of Pd and Pd/SiO_2. They concluded that the particle size and the thickness of the coating can be controlled by manipulating the relative rates of the hydrolysis and condensation reaction of TEOS.

Span-Tween 80, a commercial mixture of sorbitol monooleate and polysorbate 80, was used to prepare TiO_2 nanoparticles in microemulsions (Zhand and Gao, 2002). Polyoxyethylene 4 lauryl ether was used to prepare Pd, Pt and Pt/Pd nanoparticles, which showed a high catalytic activity (Yashima et al., 2003). Polyoxyethylene 15 cetyl ether was used by Tago et al. (2003) as a surfactant to obtain SiO_2-coated CeO_2 nanoparticles. They observed that this type of particle-forming agents affects the efficiency of silica coating on the CeO_2 nanoparticles.

Epikuron 170 a lecithin (min 67% phosphatidylcholine) used as a surfactant to prepare nimesulide, a molecule of pharmaceutical interest (Debuigne et al., 2001). The size seems to be independent of either the water: surfactant ratio or the concentration of the active compound. Debuigne et al. (2001) proposed that the constancy of the size suggesting that the size is controlled by thermodynamic stabilization of the nanoparticles with the surfactant molecules. In several important applications, ionic surfactants are used in conjunction with a co-surfactant such as a medium chain-length alcohol. The co-surfactant is an uncharged entity and its adsorption is not impeded by the electric field. It therefore provides the additional lowering of interfacial tension necessary for microemulsion formation. Co-surfactants are usually alcohols or amines ranging from C4 to C10 and helps in the formation and stabilization of micelles/microemulsions. In many cases it also acts

as an organic solvent. The co-surfactant provides a "dilution effect" in addition to that of the surfactant and causes a further decrease of the interfacial tension. If salt is added to the solution, the surface potential is partly neutralized. This decreases the coulombic repulsion between adjacent head groups and allows the formation of larger micelle. Their short hydrophobic chain and terminal hydroxyl group are known to enhance the interaction with surfactant monolayers at the interface, which can influence the curvature of the interface and internal energy. The amphiphilic nature of co-surfactants could also enable them to distribute between the aqueous and oil phase (Bose and Saha, 2003). Marchand et al. (2003) have studied the synthesis of MoS_x particles in AOT/water/n-heptane microemulsions (Marchand et al., 2003). In a Similar work Bagwe and Khilar (1997a,b) have used NP-5 as a cosurfactant to synthesise Ag particles in AOT/*n*-heptane/water.

10.2. Water content

This effect has been reviewed extensively elsewhere (Pileni, 2001, 2003, 2007; Lopez-Quintela et al., 2004). In most papers, water content is described by the water to surfactant molar ratio w^0 = ([H_2O]/[surfactant]), however it is important to recognize that the total water in the system can be raised not only by raising w^0 but also by increasing [surfactant] at constant w^0 levels (Kimijima and Sugimoto, 2005). Another effect of changing w^0 is to vary the effective concentration of reagents inside the micelles, if the overall reagent concentration is kept constant. Many papers show the final particle size to be dependent on the initial w^0 (Nanni and Dei, 2003; Berkovich et al., 2002; Lemyre and Ritcey, 2005), demonstrating control over the outcomes of the synthesis merely by changing w^0. It is also generally observed that the size of the nanocrystals produced differs from that of the initial nanoreactors and also the variation in particle size with w^0 is strongly dependent on the nature of the chemical reaction. This observation is generally attributed to a templating effect on nanocrystal growth by the reverse micelles. Unfortunately in many cases, the same effect is not seen (Kitchens et al., 2003; Krauel et al., 2005). Kitchens et al. (2003) found that, at any given value of w^0 the same size nanoparticles can be synthesized if left for sufficient time for the reaction to go to completion. They proposed that the rate of nanoparticle growth is affected by varying w^0. Surfactants are fully hydrated at given water content and increase in the water content induces formation of a thermodynamically stable emulsion made of several phases with interconnected cylinders trapped inside an onion phase and filling the interstices between spherulites (Pileni, 2001). With the water bound, the micelle interface is said to be "rigid", lowering intermicellar exchange and thus growth rates. As w^0 is raised, the film becomes more fluid, so the rate of growth increases, until it reaches a point when all extra water added is just added to the bulk water pool (at around w^0 = 10–15). At this point the extra water added merely dilutes the reagents, decreasing reaction rates, so any increase in rate of intermicellar exchange from this point is negated, and in some cases a decrease in particle size is observed (Krauel et al., 2005). These ideas and findings run contrary to the bulk of other work (Kimijima and Sugimoto, 2005; Nanni and Dei, 2003) which suggests that particle size can indeed be controlled by w^0.

10.3. Reagent concentration

Several studies have shown an increase in particle size goes hand-in-hand with reactant concentration (Lisiecki and Pileni, 2003). The clearest example is from the work of Lisiecki and Pileni (2003), who investigated the size of silver nanodisks generated as a function of the concentration of added reducing agent (hydrazine). As the ratio [hydrazine]:[AOT] was increased, an increase in particle size was observed, leading to changes in optical properties of the nanoparticle dispersion. One plausible explanation is that a 'polymerisation' of AOT occurs via reaction with hydrazine to form an imine dimmer. Increasing reagent concentration also appears to reduce polydispersity. In studies by both Lisiecki and Pileni, 2003 and Eastoe and Cox, 1995 an increase in the number of particles of a similar size was noted when concentration of reagents, $NaBH_4$ and PbS, was raised.

11. Microemulsion mediated synthesis of inorganic nanomaterials

11.1. Metals

Since metals display surface catalytic properties, the synthesis of size controllable and monodisperse metal particles is of considerable importance. The reduction method is one of the most common ways to prepare metal nanoparticles through microemulsions. Platinum, palladium, rhodium and Iridium nanoparticles have been prepared using reverse micelles (Boutonnet et al., 1982a,b). H_2PtCl_6 was dissolved in CTAB/water/octanol reverse micelles. Subsequent reduction with hydrazine produced nanoparticles. Pd nanoparticles were formed by reducing $Pd(NH_2)_4Cl_2$ or K_2PdCl_4 with N_2H_4. Rhodium particles were formed by reducing $RhCl_2$ with bubbling hydrogen, whereas iridium particles could be obtained by bubbling active hydrogen through 2% Pt-Al_2O_3 at 70 °C. Ag and Au colloidal nanoparticles were successfully prepared by reducing the $AgNO_3$ and $HAuCl_4$ in water/cyclohexane/PEGDE or PEGDE/water/*n*-hexane reverse micelles, where $NaBH_4$ was used as the reducing agent (Barnickel and Wokaum, 1990). Silver and copper salts of Aerosol OT can be used for the preparation of Ag and Cu nanoparticles (Pileni and Lisiecki, 1993). Copper nanoparticles have been synthesized in the reverse micelles using hydrazine as a reducing agent. The size of Cu nanoparticles can be controlled by the water content in the reverse micelles (Pileni and Lisiecki, 1993). Gold and silver nanoparticles were also produced by reducing gold chloridetetrahydrate $HAuCl_4$ with citric acid at 80 °C for half an hour (Chen et al., 1994). Nanoparticles of other metals such as Co, Ni and metal alloys Fe–Ni, Cu_Au and Co–Ni have also been synthesized using reverse micelles (Monnoyer et al., 1995).

11.2. Preparation of metal sulphide nanoparticles

Colloidal semiconductors are attracting much interest due to their applications as enhancement of photoreactivity and photocatalysis and non-linear optical properties. The key to synthetic investigation of this kind of nanoparticles must be the careful control of semiconductor size and size distribution. The preparation method is usually applied in the preparation

of metal sulphide particles (Petit et al., 1990). CdS particles have been synthesized in AOT and triton reverse micelles with functional surfactant such as cadmium lauryl sulfate and cadmium AOT (Petit et al., 1990). The average diametere of the particles was found to depend on the relative amount of Cd^{2+} and S^{2-}. The particles obtained from AOT were smaller and more monodisperse than those from the Triton reverse micelles. Colloidal CdS was prepared in the mixed sodium AOT/cadmium AOT/isooctane reverse micelle (Petit et al., 1990). Pbs nanoparticles can be made by mixing Polyoxethylene dodecyl erther-*n*-hexane reverse micelle, which supplies Pb^{2+} from electrolytes such as $Pb(NO_3)_2$ or $Pb(ClO_4)_2$ and other reverse micelle that contains S^{2-} and Na_2S or H_2S. A number of nanoparticle semiconductors such as CdS, PbS, CuS, Cu_2S and CdSe (Petit et al., 1990; Eastoe and Warne, 1996; Robinson et al., 1991; Haram et al., 1996) have also been synthesized using this method. In recent years apart from synthesis of nanoparticles, surface modification of the metal sulphide particles has attracted much interest. The modification of the semiconductor surface is also very important either from the point of view of enhancing the stability of the nanoparticles or for providing unique physical and chemical properties. An additional profit from this treatment is that it allows the particles to be separated from the micellar solution and redispersed in another solvent. Some surface capped semiconductor nanoparticles have been synthesized with the capping agent such as sodium hexamephosphlate and phenyl trimethylselenium (Petit et al., 1990; Harron et al., 1990).

11.3. Preparation of nanoparticles of metal salts

Many metal salts such as silver halide, metal sulphate and metal carbonate possess unique properties. Precipitation methods are usually used to prepare the nanoparticles of these materials. Silver halide nanoparticles were synthesized by reacting $AgNO_3$ with sodium halides in Aerosol OT W/O microemulsions (Chew et al., 1990). However the metal carbonate nanoparticles such as $BaCo_3$, $CaCo_3$ and $SrCO_3$ were prepared by bubbling CO_2 through the reverse micelle solution containing the corresponding aqueous metal hydroxides. Nanoparticles of AgCl and AgBr have been synthesized using reverse micelles (Bagwe and Khilar, 1997a,b; Monnoyer et al., 1995).

11.4. Metal oxides

Nanoparticles of metal oxides are usually produced by the hydrolysis method in which metal alkoxide react with water droplets in the reverse micelles. Nanoparticles of metal oxides such as ZrO_2, TiO_2, SiO_2, GeO_2 and Fe_2O_3 (Chang et al., 1994; Esquena et al., 1997; Lopez-Perez et al., 1997; Chen et al., 2008) have been synthesized. GeO_2 nanopartices can be direcly obtained from AOT-cyclohexane W/O microemulsions. SiO_2 nanoparticles could be obtained by adding $Si(OC_2H_4)_4$ to the solubilized ammonia aqueous solution in AOT and Ployoxyethylated nonulphenyl ether W/O microemulsions. Similarly ZrO_2 nanoparticles have been obtained by hydrolyzing $Zr(OC_4H_9)_4$ with sulphuric acid in ployoxyethylene nonylphenyl ether cyclohexane systems and then washed with ammonia aqueous solution. TiO_2 nanoparticles can be prepared by adding benzene solution of $TiCl_4$ to etylbenzyldimethylammonium chloride-benzene W/O microemulsions.

11.5. Preparation of magnetic nanoparticles

The first magnetic nanoparticles formed in micelles were from the oxidation of Fe^{2+} salts to form Fe_3O_4 and *c*-Fe_2O_3 (Inouye et al., 1982). This reaction was carried out in an AOT/isooctane system and formed spherical nanoparticles with surprisingly tight size distributions of less than 10%. Later, other reactions using hydrogen peroxide were used to form $MnFe_2O_4$. The initial reaction conditions not only controlled the particle size, but also the cation occupancy (Carpenter et al., 1999a,b). An interesting phenomenon seen with iron reductions is the influence of the surfactant on the iron crystal structure. If anionic surfactants (such as AOT) are used, a-Fe is formed with the body centered cubic (bcc) crystal structure expected from thermodynamic equilibrium of the bulk metal at room temperature (Duxin et al., 1997). Conversely, if a non-ionic surfactant is used (for instance, nonyl phenol polyethoxylate), a face centered cubic (fcc) crystal structure forms (Wilcoxon and Provencio, 1999). The process for the formation of metals can be expanded to form metal alloys. Instead of using a single metal salt, mixed metal salts are used and reduced simultaneously (Tanori et al., 1995). It is essential that the reduction is carried out simultaneously or mixed phase products will be formed. The precipitation of precursors that are subsequently fired to produce an oxide end product is an important synthetic process. This has been used in the synthesis of many different ferrite materials $(Mn,Zn)Fe_2O_4$, $(Ni,Zn)Fe_2O_4$, $ZnFe_2O_4$ and $BaFe_{12}O_{19}$ (Yener and Giesche, 2001; Agnoli et al., 2001). In these cases, the particles were formed with sizes between 5 and 50 nm. The particles had spheroidal morphology with typical size variations of 10%, although higher conversion temperatures generally widen the size distribution to 10–20%. The reaction time of the metathesis reaction controlled the morphology and size of the particles for this reaction. Particles synthesized by quenching the reaction after short reaction times developed polyhedral morphology and 13 nm average particle size. Similar reactions carried out for 2 h resulted in particles with spherical morphology and 39 nm average grain diameters (Carpenter et al., 1999a,b). Cobalt hexacyanoferrate nanocubes have been prepared using reverse micelles and AOT (Vaucher et al., 2002). Although there are many examples of inverse micelles used as microreactors, there are only a few examples of the use of direct micelles. Sodium dodecylsulphate is the principle surfactant used in these reactions due to the morphology of the aggregate. The most striking example of direct micelle synthesis was presented by Liu and co-workers with the synthesis of $CoFe_2O_4$ (Liu et al., 2000a,b). In this example, a chemometric model was created for predicting the size of a ferrite from the synthesis conditions of surfactant concentration, metal concentration, base concentration, and temperature. The synthesis was later expanded to include the mixed ferrites of $MnFe_2O_4$ and $MgFe_2O_4$ (Liu et al., 2000a,b). In order to control side reactions and precipitation common to aqueous systems, micelles are formed using alcohol as the polar phase. Some workers have employed ethanol-based micelles to form $SrFe_{12}O_{19}$. In this case, $Sr(OH)_2$ has such a high solubility in water that inhomogeneous and strontium deficient precipitates were formed, thus the change to ethanol was necessary. The particles display a large size distribution and a plate like morphology with an average particle size of 100 nm.

11.6. Nanowires

The Nanoparticles fabricated in the reverse micelles are spherical particles in most cases. However, since the optical, electric, and other properties of nanoparticles are affected by the shape of nanoparticles. Various shapes have been synthesized. For example, cubic pt nanoparticles have been synthesized and they showed extremely good catalysis selectivity and activity (Ahmad et al., 1996). Addition of CdS nanowires into the porous almunium oxide film will be of potential use in photo-electronics (Routkevitch et al., 1996). Qi et al. (1997) using reverse micelles of TX-100/hexanol-cyclohexane/water have successfully synthesized cubic $BaSO_4$ nanoparticles. They have found that the water content in the reverse micelles greatly affected the shape of the nanoparticles. Cubic nanoparticles of $BaSO_4$ were obtained in the higher content of water. On the other hand, in the non-ionic reverse micelle $C_{12}E_4$/cyclohexane, adding 0.1 M $BaCl_2$ and Na_2CO_3 aqueous solution to 0.2 M $C1_2E_4$/cyclohexane solution, and mixing the two reverse micelles, $BaCO_3$ nanowires were obtained. Hopwood and Mann have also synthesized $BaSO_4$ nanowires using reverse micelles (Hopwood and Mann, 1997).

11.7. Nanocomposites

Composite nanoparticles are composed of two kinds of nanoparticles, not only modifying the properties of single semiconductor nanoparticles, but also producing some new electric and optic properties. The composite semiconductor nanoparticles can be divided into sandwich type and shell-core type. Sandwich type CdS–TiO_2 (Lawless et al., 1995) and CdS–SnO_2 have been prepared and show prospects in solar cell applications (Nasr et al., 1997). On the other hand, shell-core type composite nanoparticles such as CdS–ZnS (Hirai et al., 1994) CdS/PbS CdS/HgS (Kamalov et al., 1996; Hota et al., 2007) CdS/Ag_2S (Han et al., 1998) CdS/CdSe, CdSe/ZnS (Peng et al., 1997; Kortan et al., 1990), CdSe/ZnSe have been synthesized using different methods (Han et al., 1998). They showed enhancement of photocatalytic efficiency and strong enhancement of emission. Reverse micelle is also an important method for synthesizing the composite nanoparticles. So far reverse micelles have been successfully used to synthesize composite nanoparticles such as CdS–ZnS, CdS–Ag_2S and CdSe–ZnS, CdSe–ZnSe (Han et al., 1998; Peng et al., 1997). For core shell nanoparticles the synthesis contains two steps; the first step is the formation of core nanoparticles in the reverse micelles and the second step is the growth of the shell particle on the core. CdS/ZnS (where CdS is the core and the ZnS is the shell) are the typical shell core type composite nanoparticles and can be synthesized as follows. Mixing of the reverse micelles containing Cd^{2+} and S^{2-} in a 1:2 ratio, one can obtain the core CdS reverse micelle solution. In this reverse micelle S^{2-} is excess. After several minutes, Zn^{2+} containing reverse micelle was added. ZnS precipitated in the core CdS nanoparticles, and a shell-Core type CdS/ZnS composite nanoparticle was obtained. Using this method, composite nanoparticles of CdS/ZnS and ZnS/CdS have been synthesized. Another type of composite nanoparticle contains two metals not in the 1:1 ratio have also been reported. Chen and Chen (2002) have reported the synthesis of Au–Ag, Au–Pd and Pd–Pt bimetallic nanoparticles in water/AOT/isooctane microemulsions (Chen and Chen, 2002; Wu et al., 2001a,b). The following mechanism is proposed: for Au–Ag (Chen and Chen, 2002) and Au–Pd (Wu et al., 2001a,b), the reduction rate is so large that almost all of the ions are reduced before the formation of nuclei. Then, the atoms start to aggregate to form the nuclei. Since the nucleation rate of Au is much faster than that of Ag (Chen and Chen, 2002) or Pd (Wu et al., 2001a,b), the nuclei of the bimetallic system should be mainly formed from Au atoms, and the composition of the nuclei might have a higher Au concentration than that of the feeding solution, i.e., Au might act as the seed for the formation of the bimetallic particle. All nuclei might be formed almost at the same time. After that, Ag or Pd atoms codeposite on to the nuclei and grow to their final sizes. The faster growth rate of Au than Ag or Pd leads to the enrichment of Ag or Pd in the outer layer of the bimetallic nanoparticle. For the case of Pd–Pt (Wu et al., 2001a,b), the formation rate of Pd nanoparticles is faster than Pt nanoparticles, but the difference is less than Au–Ag and Au–Pd particles. Consequently, the nucleus might contain both Pd and Pt codeposited at a similar deposition rate, so that a homogeneous alloy structure is obtained. It is interesting to note that the same Pd–Pt synthesis using a different reduction agent i.e., different chemical reaction, leads to a different final nanoparticle size.

12. Microemulsion mediated synthesis of organic nanomaterials

Only a limited number of organic nanoparticles can be prepared using oil in water microemulsions usually called microemulsion polymerization (Vaucher et al., 2002). Phase separation is perhaps the main reason why such techniques made little progress within the past decade (Holdcroft and Guillet, 1990). Nanosize polymer particles can be obtained using polymerization reactions in o/w microemulsions, this leads to hydrophobic nanoparticles (10–40 nm) dispersed in water (Candau, 1990). The advantage of this method is fast polymerization rates and high molar mass of polymers, while the drawback is the need of high weight ratio of surfactant to polymer.

The first successful microemulsion polymerization was reported by Atik and Thomas (1981b) who used CTAB/styrene/hexanal/water O/W microemulsion. The reaction was carried out either thermally using azobisisobutyronitrile (AIBN) or radiolytically using Cs γ-ray source. Monodisperse latex nanoparticles of diameters 35 and 20 nm were obtained. Styrene has also been polymerized using three component microemulsions of dodecyl trimethyl ammonium bromide (DTAB) and potassium persulphate (KPS) initiator (Perez-Luma et al., 1990). This resulted in monodisperse lattices with radii in the range of 20–30 nm. Guo et al. (1989) studied styrene polymerization in SDS/pentanol/water microemulsions using both water soluble KPS and oil soluble AMBN as initiators and found that the fraction of formed particles were determined by the amount of initiator. Palani et al. (1991) studied the polymerization of MMA using MMA/ethylene glycol dimethacrylate/water system with acylamide as amphiphile. The particles formed were transparent up to 60% of water in the microemulsion systems.

Different microemulsion systems have been used to synthesize organic nanoparticles of cholesterol, Retinol Rhodiarome, Rhovanil (Destree and Nagy, 2006). The microemulsions used are AOT/heptane/water, Triton/decanol/water, and CTABr/hexanol/water. The general preparation of these organic

nanoparticles consists of the direct precipitation of the active compound in the aqueous cores of the microemulsion. After their preparation, nanoparticles are revealed with iodine vapor and observed with a transmission electron microscope (The mechanism of the formation of nanoparticles has been previously studied (Nagy and Mittal, 1999). This consists of several stages. The solution of the active compound in an appropriate solvent penetrates inside the aqueous cores by crossing the interfacial film. The solvent certainly plays a role in the transport of the active compound inside the aqueous cores. The active compound precipitates in the aqueous cores because of its insolubility in water, and the nuclei are thus formed. The so formed nuclei can grow because of the exchange of the active compound between the aqueous cores. Finally, the nanoparticles are stabilized by the surfactants.

12.1. Synthesis of nanoparticles of pharmaceutical interest

Solid nanoparticles of nimesulide (molecule of a pharmaceutical interest) have been synthesized by direct precipitation in two water/oil (W/O) microemulsion systems Epikuron 170 (E170, which is a lecithin)/isopropyl myristate/water/*n*-butanol (ME1) and E170/isopropyl myristate/water/isopropanol (ME2). The size distributions of the observed nanoparticles are relatively narrow for the two systems. In the two microemulsions, the diameter of the nanoparticles is between 45° and 60 A°. The interest in these organic nanoparticles lies in their pharmaceutical applications (Debuigne et al., 2001). First, the microemulsions used to synthesize the nanoparticles are potential systems for drug delivery (Lawrence, 1994). Indeed, microemulsions have a low viscosity, making intravenous injections easier. Second, the solid organic substances could be injected directly into the vena in the form of nanoparticles. As these substances are often insoluble in water, a classical method of drug delivery using aqueous solutions is not applicable. However, if nanoparticles could be prepared in suspension in water, they could be directly injected. The size of the particles is very important, because bigger particles could lead to embolism. In yet another study solid nanoparticles of Amoxicillin has been reported. Three different types of amoxicillin nanostructures were synthesized successfully (Xike et al., 2005). It is conceivable that these special nanostructures can enhance the solubility rate of dissolution, and bioactivity of amoxicillin (Horn and Rieger, 2001).

13. Conclusions

The long-term objective of this study is to create the experimental and theoretical Know-How for the large-scale realization of a process for the synthesis of tailored nanoparticles by precipitation in microemulsion droplets. The technical-scale production of nanoparticles with tailored properties is of particular interest due to the increasing demand from industry. This study provides the basis for the scale-up of the synthesis route in water-in-oil (W/O)-microemulsion droplets. However research in this field is still in infancy and efforts are needed for better understanding.

References

Ahmad, T.D., Wang, Z.L., Hengiein, A., Sayed, M.A., 1996. Cubic colloidal platinum nanoparticles. Chem. Mater. 8, 1161–1163.

Ahmad, N., Malik, M.A., Al-Nowaiserb, F.M., Khan, Z., 2010. A kinetic study of silver nanoparticles formation from paracetamol and silver(I) in aqueous and micellar media. Colloid. Surf. B: Biointerf. 78, 109–114.

Agnoli, F., Zhou, W.L., Connor, C.J.O., 2001. Synthesis of cubic antiferromagnetic $KMnF_3$ nanoparticles using reverse micelles and their self-assembly. Adv. Mater. 13, 1697–1699.

Alejandra, L., Reinhard, S., 2006. Synthesis of manganite perovskite $Ca_{0.5}Sr_{0.5}MnO_3$ nanoparticles in w/o-microemulsion. Mater. Res. Bull. 41, 333–339.

Althues, H., Kaskel, S., 2002. Sulfated zirconia nanoparticles synthesized in reverse microemulsions: preparation and catalytic properties. Langmuir 18, 7428–7435.

Andersson, M., Sterlund, L., Ljungstro, S., Palmqvist, A., 2002. Preparation of nanosize anatase and rutile TiO_2 by hydrothermal treatment of microemulsions and their activity for photocatalytic wet oxidation of phenol. J. Phys. Chem. B 106, 674–679.

Anderson, M.T., Martin, J.E., Odinek, J., Newcomer, P., 2006. Synthesis of surfactant-templated mesoporous materials from homogeneous solutions. Access in Nanoporous Mater., 29–37.

Atik, S.S., Thomas, J.K., 1981a. Transport of ions between water poles in alkanes. Chem. Phys. Lett. 79, 351–354.

Atik, S.S., Thomas, J.K., 1981b. Polymerized microemulsions. J. Am. Chem. Soc. 103, 4279–4280.

Ayyup, P., Multani, M., Barma, M., Palkar, V.R., Vijayaraghavan, R., 1988. Size induced Structural phase transitions and hyperfine properties of microcrystalline Fe_2O_3. J. Phys. C: Solid State Phys. 21, 2229–2245.

Bae, D.S., Han, K.S., Adair, J.H., 2002. Synthesis and microstructure of Pd/SiO_2 nanosized particles by reverse micelle and sol/gel processing. J. Mater. Chem. 12, 3117–3120.

Bagwe, R.P., Khilar, K.C., 2000. Effects of intermicellar exchange rate on the formation of silver nanoparticles in reverse microemulsions of AOT. Langmuir 16, 905–910.

Bagwe, R.P., Khilar, K.C., 1997a. Effects of the intermicellar exchange rate and cations on the size of silver chloride nanoparticles formed in reverse micelles of AOT. Langmuir 13, 6432–6438.

Bagwe, R.P., Khilar, K.C., 1997b. Effects of intermicellar exchange rate on the formation of silver nanoparticles in reverse microemulsions of AOT. Langmuir 13, 6432–6438.

Barnickel, P., Wokaum, A., 1990. Synthesis of metal colloids in inverse microemulsions. Mol. Phys. 69, 1–9.

Bandyopadhyaya, R., Kumar, R., Gandhi, K.S., Ramkrishna, D., 1997. Modeling of precipitation in reverse micellar systems. Langmuir 13, 3610–3620.

Bandyopadhyaya, R., Kumar, R., Gandhi, K.S., Ramkrishna, D., 2000. Simulation of precipitation reactions in reverse micelles. Langmuir 16, 7139–7149.

Bandow, S., Kimura, K., Konno, K., Kitahara, A., 1987. Magnetic properties of magnetite ultrafine particles prepared by W/O microemulsion method. Jpn. J. Appl. Phys. 26, 713–717.

Berkovich, Y., Aserin, A., Wachtel, E., Garti, N., 2002. Preparation of amorphous aluminum oxide-hydroxide nanoparticles in amphiphilic silicone-based copolymer microemulsions. J. Colloid. Interf. Sci. 245, 58–67.

Bose, S., Saha, S.K., 2003. Synthesis and characterization of hydroxyapatite nanopowders by emulsion technique. Chem. Mater. 15, 4464–4469.

Boutonnet, M., Kizling, J., Stenius, P., Maire, G., 1982a. The preparation of monodisperse colloidal metal particles from microemulsions. Colloid. Surf. 5, 209–225.

Boutonnet, M., Kizling, J., Stenius, P., Maire, G., 1982b. The preparation of monodisperse colloidal metal particles from microemulsions. Colloid. Surf. 5, 209–225.

Brigger, I., Dubernet, C., Couvreur, P., 2002. Nanoparticles in cancer therapy and diagnosis. Adv. Drug Deliver. Rev. 54, 631–651.

Candau, F., 1990. In Scientific Methods for the Study of Polymer Colloids and their Applications, Kluwer Academic Publ., Dorrecht, The Netherlands, p. 73.

Carpenter, E.E., Connor, C.J.O., Harris, V.G., 1999a. Atomic structure and magnetic properties of $MnFe_2O_4$ nanoparticles produced by reverse micelle synthesis. J. Appl. Phys. 85, 5175–5177.

Carpenter, E.E., Sangregroio, C., Connor, C.J.O., 1999b. Synthesis of antiferromagnetic macromolecular particles. Mol. Cryst. Liq. Cryst. 334, 641–649.

Chan, W.C.W., Maxwell, D.J., Gao, X., Bailey, R.E., Han, M., Nie, S., 2002. Luminescent quantum dots for multiplexed biological detection and imaging. Curr. Opin. Biotechnol. 13, 40–46.

Chang, S.Y., Liu, L., Asher, S.A., 1994. Preparation and properties of tailored morphology, monodisperse colloidal silica-cadmium sulfide nanocomposites. J. Am. Chem. Soc. 116, 6739–6744.

Chen, D.H., Wu, S.H., 2000. Synthesis of nickel nanoparticles in water in oil microemulsions. Chem. Mater. 12, 1354–1360.

Chen, J.P., Lee, K.M., Sorensen, C.M., Klabunde, K.J., Hadjipanaysis, G.C., 1994. Magnetic properties of microemulsion synthesized cobalt fine particles. J. Appl. Phys. 75, 5876–5878.

Chew, C.H., Gan, L.M., Shah, D.O., 1990. The effect of alkanes on the formation of ultrafine silver bromide particles in ionic w/o microemulsions. J. Dispersion Sci. Technol. 11, 593–609.

Chen, M., Wu, Y., Zhou, S., Wu, L., 2008. Shape-controllable synthesis of crystalline Ni complex particles via AOT-based microemulsions. J. Phys. Chem. B 112, 6536–6541.

Chen, D.H., Chen, C.J., 2002. Formation and characterization of Au-Ag bimetallic nanoparticles in water-in-oil microemulsions. J. Mater. Chem. 12, 1557–1562.

Chhabra, V., Free, M.L., Kang, P.K., Truesdail, S.E., Shah, D.O., 1997. Microemulsion as an emerging technology. Tensile Surfact. Det. 34, 156–168.

Chou, K.S., Ren, C.Y., 2000. Synthesis of nanosized silver particles by chemical reduction method. Mater. Chem. Phys. 64, 241–246.

Cushing, B.L., Kolesnichenko, V.L., Connor, C.J.O., 2004. Recent advances in the liquid-phase syntheses of inorganic nanoparticles. Chem. Rev. 104, 3893–3946.

Debuigne, F., Cuisenaire, J., Jeunieau, L., Masereel, B., Nagy, J.B., 2001. Synthesis of nimesulide nanoparticles in the microemulsion epikuron/isopropyl myristate/water/*n*-butanol (or isopropanol). J. Colloid. Interf. Sci. 243, 90–101.

Destree, J., Nagy, B., 2006. Mechanism of formation of inorganic and organic nanoparticles from microemulsions. Adv. Colloid. Interf. Sci. 123, 353–367.

Destree, C., Debuigne, F., George, S., Champagne, B., Guillaume, M., Ghijsen, J., Nagy, J.B., 2008. J complexes of retinol formed within the nanoparticles prepared from microemulsions. Colloid. Polym. Sci. 286, 1463–1470.

Dong-Hwang, C., Szu-Han, W., 2003. Synthesis and characterization of nickel nanoparticles by hydrazine reduction in ethylene glycol. J. Colloid. Interf. Sci. 259, 282–286.

Duxin, N., Stephan, O., Petit, C., Bonville, P., Colliex, C., Pileni, M.P., 1997. Pure α-Fe coated by an $Fe_{1-x}B_x$ alloy. Chem. Mater. 9, 2096–2100.

Eastoe, J., Cox, A.R., 1995. Formation of PbS nanoclusters using reversed micelles of lead and sodium Aerosol-OT. Colloid. Surf. A Physicochem. Eng. Asp. 101, 63–76.

Eastoe, J., Warne, M., 1996. Nanoparticles and polymer synthesis in microemulsions. Curr. Opin. Colloid. Interf. Sci. 1, 800–805.

Ekwall, P., Mandell, L., Solyom, P., 1970. The solution phase with reversed micelles in the cetyltrimethylammonium bromide-hexanol-water system. J. Colloid. Interf. Sci. 35, 266–272.

Esquena, J., Tadros, T.F., Kostareios, K., Solans, C., 1997. Preparation of narrow size distribution silica particles using microemulsions. Langmuir 13, 6400–6406.

Fang, X., Yang, C., 1999. An experimental study on the relationship between the physical properties of CTAB/hexanol/water reverse micelles and ZrO2_Y2O3 nanoparticles prepared. J. Colloid. Interf. Sci. 212, 242–251.

Fang, J., Stokes, K.L., Wiemann, J.A., Zhou, W.L., Dai, J., Chen, F., Connor, C.J.O., 2001. Microemulsion-processed bismuth nanoparticles. Mater. Sci. Eng. B 83, 254–257.

Fletcher, P.D.I., Robinson, B.H., Tabony, J., 1986. A quasi-elastic neutron scattering study of water-in-oil microemulsions stabilised by aerosol-OT. Effect of additives including solubilised protein on molecular motions. J. Chem. Soc. Faraday Trans. I 82, 2311–2321.

Giannakas, A.E., Vaimakis, T.C., Ladavos, A.K., Trikalitis, P.N., Pomonis, P.J., 2003. Variation of surface properties and textural features of spinel ZnAl2O4 and perovskite LaMnO3 nanoparticles prepared via CTAB–butanol–octane–nitrate salt microemulsions in the reverse and bicontinuous state. J. Colloid. Interf. Sci. 259, 244–253.

Goncalves, S.A.P., De Pauli, S.H., Tedesco, A.C., Quina, F.H., Okano, L.T., Bonilha, J.B.S., 2003. Counterion exchange selectivity coefficients at water-in-oil microemulsion interface. J. Colloid. Interf. Sci. 267, 494–499.

Guo, J.S., El-Aasser, M.S., Vanderhoff, J.W., 1989. Microemulsion polymerization of styrene. J. Polym. Sci. Part A: Polym. Chem. 27, 691–710.

Hanaoka, T., Hayashi, H., Tago, T., Kishida, M., Wakabayashi, K., 2001. In situ immobilization of ultrafine particles synthesized in a water/oil microemulsion. J. Colloid. Interf. Sci. 235, 235–240.

Han, M.Y., Huang, W., Chew, C.H., Gan, L.M., Zhang, X.J., Ji, W., 1998. Large nonlinear absorption in coated ag2s/cds nanoparticles by inverse microemulsion. J. Phys. Chem. B 102, 1884–1887.

Harron, N., Wang, Y., Eckert, H., 1990. Synthesis and characterization of surfaced capped size quantized CdS cluster: chemical control of cluster size. J. Am. Chem. Soc. 112, 1322–1323.

Haram, S.K., Mahadeshwar, A.R., Dixit, S.G., 1996. Synthesis and characterization of copper sulphate nanoparticles in triton-X 100 water-in-oil microemulsion. J. Phys. Chem. 100, 5868–5873.

Hirai, T., Shiojiri, S., Komasawa, I., 1994. Preparation of metal sulfide composite ultrafine particles in reverse micellar systems and their photocatalytic property. J. Chem. Eng. Jpn. 27, 590–597.

Hirai, H., Sato, H., Komasawa, I., 1993. Mechanism of formation of titanium dioxide ultrafine particles in reverse micelles by hydrolysis of titanium tetrabutoxide. Ind. Eng. Chem. Res. 32, 3014–3019.

Holdcroft, Y.S., Guillet, J.E., 1990. Microemulsion polymerization of styrene: a study using pulsed laser initiation. J. Polym. Sci.: Polym. Chem. Ed. 28, 1823–1829.

Holmes, J.D., Lyons, D.M., Ziegler, K.J., 2003. Supercritical fluid synthesis of metal and semiconductor nanowires. Chem. Eur. J. 9, 2144–2150.

Hopwood, J.D., Mann, S., 1997. Synthesis of barium sulfate nanoparticles and nanofilaments in reverse micelles and microemulsions. Chem. Mater. 9, 1819–1828.

Horn, D., Rieger, J., 2001. Organic nanoparticles in aqueous phase. Angew Chem. Int. Ed. 40, 4330–4361.

Hota, G., Idage, S.B., Khilar, K.C., 2007. Characterization of nanosized CdS–Ag_2S core-shell nanoparticles using XPS technique. Colloid. Surf. A: Physicochem. Eng. Asp. 293, 5–12.

Hou, M.J., Shah, D.O., 1988. Interfacial phenomena in biotechnology and materials processing. In: Attia, Y.A. (Ed.), Elsevier, Amsterdam, p. 443.

Hu, A., Yao, Z., Yu, X., 2009. Phase behavior of a sodium dodecanol allyl sulfosuccinic diester/*n*-pentanol/methyl acrylate/butyl acrylate/water microemulsion system and preparation of acrylate latexes by microemulsion polymerization. J. Appl. Polym. Sci. 113, 2202–2208.

Hungrıa, A.B., Martınez-Aries, A., Fernandez-Garcıa, M., Iglesias-Juez, A., Guerrero-Ruiz, A., Calvino, C.C., ConesaSoria, J.C.J., 2003. Structural, morphological and oxygen handling properties of nanosized cerium–terbium mixed oxides prepared by microemulsions. Chem. Mater. 15, 4309–4316.

Inouye, K., Endo, R., Otsuka, Y., Miyashiro, K., Kaneko, K., Ishikawa, T., 1982. Oxygenation of ferrous ions in reversed micelle and reversed microemulsion. J. Phys. Chem. 86, 1465–1469.

Jain, R., Mehra, A., 2004. Monte-Carlo models for nanoparticle formation in two microemulsion systems. Langmuir 20, 6507–6513.

Julian, E., Martin, J., Hollamby, Laura, H., 2006. Recent advances in nanoparticle synthesis with reversed micelles. Adv. Colloid. Interf. Sci. 128, 5–15.

Kamalov, V.F., Little, R., Logunov, S.L., El-Sayed, M.A., 1996. Picosecond electronic relaxation in CdS/HgS/CdS quantum dot quantum well semiconductor nanoparticles. J. Phys. Chem. 100, 6381–6384.

Kimijima, K., Sugimoto, T.J., 2005. Effects of the water content on the growth rate of AgCl nanoparticles in a reversed micelle system. Colloid. Interf. Sci. 286, 520–525.

Kitchens, C.L., McLeod, M.C., Roberts, C.B., 2003. Solvent effects on the growth and steric stabilization of copper metallic nanoparticles in AOT reverse micelle systems. J. Phys. Chem. B 107, 11331–11338.

Kortan, A.R., Hull, R., Opila, R.L., Bawendi, M.G., Steigerwald, M.L., Carroll, P.J., Bres, L.E., 1990. Nucleation and growth of CdSe on ZnS quantum crystallite seeds, and viece verca, in inverse micelle media. J. Am. Chem. Soc. 112, 1327–1332.

Koumoudilis, G.C., Katsoulidis, A.P., Ladavos, A.K., Pomonis, P.J., Trapalis, A.T., Vaimakis, T.C., 2003. Preparation of hydroxyapatite via microemulsion route. J. Colloid. Interf. Sci. 259, 254–260.

Krauel, K., Davies, N.M., Hook, S., Rades, S.S., 2005. Using different structure types of microemulsions for the preparation of poly(alkylcyanoacrylate) nanoparticles by interfacial polymerization. J. Control Release 106, 76–87.

Kresge, C.T., Leonowicz, M.E., Roth, W.J., Virtula, J.C., Beck, J.S., 1992. Ordered mesoporous molecular sieves synthesized by a liquid-crystal template mechanism. Nature 359, 710–712.

Kumar, A.R., Hota, G., Mehra, A., Khilar, K.C., 2004. Modeling of nanoparticles formation by mixing of two reactive microemulsions. AIChE J. 50, 1556–1567.

Kurihara, K., Kizling, J., Stenius, P., Fendler, J.H., 1983. Laser and pulse radiolytically induced colloidal gold formation in water-in-oil microemulsions. J. Am. Chem. Soc., 2574–2579.

La Mer, V.K., Dinegam, R.H., 1950. Theory, production and mechanism of formation of monodispersed hydrosols. J. Am. Chem. Soc. 72, 4847–4854.

Lal, M., Chhabara, V., Ayyub, P., Maitra, M.A., 1998. Preparation and characterization of ultrafine TiO_2 particles in reverese micelles by hydrolysis of Ti-DEHSS. J. Mater. Res. 13, 1249–1254.

Lawless, D., Kapoor, S., Meisel, D., 1995. Bifunctional capping of CdS nanoparticles and bridging to TiO_2. J. Phys. Chem. 99, 10329–10335.

Lawrence, M.J., 1994. Surfactatnt systems-microemulsions and vesicles as vehicles for drug delivery. Eur. J. Drug Metab. Pharmacokin. 3, 257–269.

Lemyre, J.L., Ritcey, A.M., 2005. Synthesis of lanthanide fluoride nanoparticles of varying shape and size. Chem. Mater. 17, 3040–3043.

Li, Y.C., Park, C.W., 1999. Particle size distribution in the synthesis of nanoparticles using microemulsions. Langmuir 15, 952–956.

Li, Y., Kim, N., Lee, E.J., Cai, W.P., Cho, S.O., 2006. Synthesis of silver nanoparticles by electron irradiation of silver acetate. Nucl. Inst. Methods Phys. Res. B 251, 425–428.

Lindman, B., Oisson, U., 1996. Structure of microemulsions studied by NMR. Ber. Bunscnges. Phys. Chem. 10, 344–364.

Lisiecki, I., Pileni, M.P., 2003. Synthesis of well-defined and low size distribution cobalt nanocrystals: the limited influence of reverse micelles. Langmuir 19, 9486–9489.

Liu, C., Zou, B.S., Rondinone, A.J., Zhang, Z.J., 2000a. Chemical control of superparamagnetic properties of magnesium and cobalt spinel ferrite nanoparticles through atomic level magnetic couplings. J. Am. Chem. Soc. 122, 6263–6267.

Liu, C., Zou, B.S., Rondinone, A., Zhang, Z.J., 2000b. Reverse micelle synthesis and characterization of superparamagnetic $MnFe_2O_4$ spinel ferrite nanocrystallites. J. Phys. Chem. B 104, 1141–1145.

Liu, Z., Lee, J.Y., Han, M., Chen, W., Gan, L.M., 2002. Synthesis and characterization of PtRu/C catalysts from microemulsions and emulsions. J. Mater. Chem. 12, 2453–2458.

Lopez-Quintela, M.A., Tojo, C., Blanco, M.C., Garcia Rio, L., Leis, J.R., 2004. Microemulsion dynamics and reactions in microemulsions. Curr. Opin. Colloid. Interf. Sci. 9, 264–278.

Lopez-Perez, J.A., Lopez-Quintela, M.A., Mira, J., Rivas, J., Charles, S.W., 1997. Advances in the preparation of magnetic nanoparticles by the microemulsion method. J. Phys. Chem. B 101, 8045–8047.

Luisi, P.L., Majid, L.J., Fendler, J.H., 1986. Solubilization of enzymes and nucleic acids in hydrocarbon micellar solution. Crit. Rev. Biochem. 20, 409–474.

Marchand, K.E., Tarret, M., Lechaire, J.P., Normand, L., Kasztelan, S., Cseri, T., 2003. Investigation of AOT-based microemulsions for the controlled synthesis of MoSx nanoparticles: an electron microscopy study. Colloid. Surf. A: Physicochem. Eng. Asp. 214, 239–248.

Monnoyer, P., Fonseca, A., Nagy, J.B., 1995. Preparation of colloidal AgBr particles from microemulsions. Colloid. Surf. A: Physicochem. Eng. Asp. 100, 233–243.

Myerson, A.S., 1983. Handbook of Industrial Crytallization. Butterworth-Heinemann, Boston, pp. 1–31.

Nagashima, K., Lee, C.T., Johnston, X., DeSimone, J.M., Johnson, C.S., 2003. NMR studies of water transport and proton exchange in water-in-dioxide microemulsions. J. Phys. Chem. B 106, 1962–1968.

Nagy, J.B., 1989. Multinuclear NMR characterization of microemulsions-preparation monodisperse colloidal metal boride particles. Colloid. Surf. 3, 201–220.

Nagy, J.B., Mittal, K.L., 1999. Handbook of Microemulsion Science and Technology. Marcel Dekker, New York, p. 499.

Nanni, A., Dei, L., 2003. $Ca(OH)_2$ nanoparticles from w/o microemulsions. Langmuir 19, 933–938.

Nasr, C., Hotchandani, S., Kim, W.Y., Schmehi, R.H., Kamat, P.V., 1997. Photoelectrochemistry of composite semiconductor thin films. Photosensitization of SnO_2/CdS coupled nanocrystallites. J. Phys. Chem. B 101, 7480–7487.

Natarajan, U., Handique, K., Mehra, A., Bellare, J.R., Khilar, K.C., 1996. Ultrafine metalparticle formation in reverse micellar systems: effects of intermicellar exchange on the formation of particles. Langmuir 12, 2670–2678.

Nersisyan, H.H., Lee, J.H., Son, H.T., Won, C.W., Maeng, D.Y., 2003. A new and effective chemical reduction method for preparation of nanosized silver powder and colloid dispersion. Mater. Res. Bull. 38, 949–956.

Nickel, U., Castell, A., Poppl, K., Schneider, S., 2000. A silver colloid produced by reduction with hydrazine as support for highly sensitive surface-enhanced Raman spectroscopy. Langmuir 16, 9087–9091.

Ohde, H., Hunt, F., Wai, C.M., 2001. Synthesis of silver and copper nanoparticles in a water-in-supercritical-carbon dioxide microemulsion. Chem. Mater. 13, 4130–4135.

Ohde, H., Ohde, M., Bailey, F., Kim, H., Wai, C.M., 2002a. Water-in-CO_2 microemulsions as nanoreactors for synthesizing CdS and ZnS nanoparticles in supercritical CO_2. Nano Lett. 2, 721–724.

Ohde, H., Wai, C.M., Kim, H., Kim, J., Ohde, M., 2002b. Hydrogenation of olefins in supercritical CO_2 catalyzed by palladium nanoparticles in water-in-CO_2 microemulsion. J. Am. Chem. Soc. 124, 4540–4541.

Ohde, M., Ohde, H., Wai, C.H., 2002. Catalytic hydrogenation of arenes with rhodium nanoparticles in a water in supercritical CO_2 microemulsion. Chem. Commun., 2388–2389.

Osseo-Asare, K., Arriagada, F.J., 1990. Proceeding of the Third International Conference on Powder Processing Science, San Diego. ISBN 0-944904-28-9.

Palani, R.W., Sasthav, W.R., Cheung, H.M., 1991. Formation of porous polymeric structures by the polymerization of single-phase microemulsions formulated with methyl methacrylate and acrylic acid. Langmuir 7, 2586–2591.

Pang, Y.X., Bao, X., 2002. Aluminium oxide nanoparticles prepared by water-in-oil microemulsions. J. Mater. Chem. 12, 3699–3704.

Pang, Q., Shi, J., Liu, Y., Xing, D., Gong, M., Xu, N., 2003. A novel approach for preparation of Y_2O_3:$Eu3^+$ nanoparticles by micro-emulsions-microwave heating. Mater. Sci. Eng. B 103, 57–61.

Peng, X., Sclamp, M.C., Kadavanich, A.V., Alivisatos, A.P., Epitaxial, A.P., 1997. Growth of highly luminescent CdSe/CdS core/shell nanocrystals with photostability and electronic accessibility. J. Am. Chem. Soc. 119, 7019–7029.

Perez-Luma, V.H., Puig, J.E., Castano, V.M., Rodriguez, B.E., Murthy, A.K., Kaler, E.W., 1990. Styrene polymerization in three-component cationic microemulsions. Langmuir 6, 1040–1044.

Petit, C., IxonL, Pileni, M.P., 1990. Synthesis of cadmium sulfide in situ in reverse micelles 2. Influence of the interface on the growth of the particles. J. Phys. Chem. 94, 1598–1603.

Pileni, M.P., 2003. Nanocrystals: fabrication, organization and collective properties. C.R. Chimie. 6, 965–978.

Pileni, M.P., 2007. Control of the size and shape of inorganic nanocrystals at various scales from nano to macrodomains. J. Phys. Chem. C 111, 9019–9038.

Pileni, M.P., 2001. Mesostructured fluids in oil rich regions: structural and templating approaches. Langmuir 17, 7476–7487.

Pileni, M.P., 2008. Supracrystals of inorganic nanocrystals: an open challenge for new physical properties. Acc. Chem. Res. 41, 1799–1809.

Pileni, M.P., 1989. Structure and Reactivity in Reverse Micelles, Ed. Elsevier, Amsterdam.

Pileni, M., Lisiecki, I., 1993. Nanometer copper metallic particles synthesis in reverse micelles. Colloids Surf. A: Physicochem. Eng. Asp. 80, 63–68.

Porta, F., Prati, L., Rossi, M., Scari, G., 2002. Synthesis of Au(0) nanoparticles from W/O microemulsions. Colloid. Surf. A: Physicochem. Eng. Asp. 211, 43–48.

Prince, L.M., 1977. Microemulsion Theory and Practice. Academic Press, New York, 177.

Qi, L.M., Ma, J., Chen, H., Zhao, Z., 1997. Reverse micelle based formation of $BaCO_3$ nanowires. J. Phys. Chem. B 101, 3460–3463.

Rauscher, F., Veit, P., Sundmacher, K., 2005. Analysis of a technical-grade w/o-microemulsion and its application for the precipitation of calcium carbonate nanoparticles. Colloid. Surf. A: Physicochem. Eng. Asp. 254, 183–191.

Robinson, B.H., Towey, T.F., Zourab, S., Visser, A.J.W.G., Van Hoek, A., 1991. Characterization of cadmium sulphide colloids in reverse micelles. Colloid. Surf. 61, 175–188.

Rodriguez, J.A., Hanson, J.C., Kim, J.Y., Liu, G., 2003. Properties of CeO_2 and Ce1-x $ZrxO_2$ nanoparticles: X-ray absorption near-edge spectroscopy, density functional and time- resolved X-ray diffraction studies. J. Phys. Chem. B 107, 3535–3543.

Routkevitch, D., Bigoni, T., Moskovits, M., Xu, J.M., 1996. Electrochemical fabrication of CdS nanowire arrays in porous anodic aluminum oxide templates. J. Phys. Chem. 100, 14037–14047.

Santra, S., Tapec, R., Theodoropoulou, N., Dobson, J., Hebard, A., Tan, W., 2001. Synthesis and characterization of silica-coated iron oxide nanoparticles in microemulsions: the effects of nonionic surfactants. Langmuir 17, 2900–2906.

Schulman, J.H., Stoekenius, W., Prince, L.M., 1959. Mechanism of formation and structure of microemulsions by electron microscopy. J. Phys. Chem. 63, 1677–1680.

Shao, K., Yao, J.N., 2006. Preparation of silver nanoparticles via a non-template method. Mater. Lett. 60, 3826–3829.

Sileikaite, A., Prosycevas, I., Puiso, J., Juraitis, A., Guobiene, A., 2006. Analysis of silver nanoparticles produced by chemical reduction of silver salt solution. Mater. Sci. 12, 4–9.

Shervani, Z., Ikushima, Y., Hakuta, Y., Kunieda, H., Aramaki, K., 2006. Effect of cosurfactants on water solubilization in supercritical carbon dioxide microemulsions. Colloid. Surf. A: Physicochem. Eng. Asp. 289, 229–232.

Sondi, I., Siiman, O., Matijevic, E., 2000. Preparation of aminodextran-CdS nanoparticle complexes and biologically active antibody-aminodextran-CdS nanoparticle conjugates. Langmuir 16, 3107–3118.

Stallings, W.E., Lamb, H.H., 2003. Synthesis of nanostructured Titania powders via hydrolysis of titanium isopropoxide in supercritical carbon dioxide. Langmuir 19, 2989–2994.

Sun, X., Luo, Y., 2005. Preparation and size control of silver nanoparticles by a thermal method. Mater. Lett. 59, 3847–3850.

Sun, Y., Xia, Y., 2002. Shape-controlled synthesis of gold and silver nanoparticles. Science 298, 2176–2179.

Sun, Y., Atorngitjawat, P., Meziani, M.J., 2001. Preparation of silver nanoparticles via rapid expansion of water in carbon dioxide microemulsion into reductant solution. Langmuir 17, 5707–5710.

Tago, T., Tashiro, S., Hashimoto, Y., Wakabayashi, K., Kishida, M., 2003. Synthesis and optical properties of SiO_2-coated CeO_2 nanoparticles. J. Nanopart Res. 5, 55–60.

Tanori, N., Duxin, C., Petit, I., Lisiecki, P., Veillet, Pileni, M.P., 1995. Synthesis of nanosize metallic and alloyed particles in ordered phases. Colloid. Polym. Sci. 273, 886–892.

Tartaj, P., Serna, C.J., 2002. Microemulsion-assisted synthesis of tunable superparamagnetic composites. Chem. Mater. 14, 4396–4402.

Tsuhi, T., Iryo, K., Watanable, N., Tsuhi, M., 2002. Preparation of silver nanoparticles by laser ablation in solution: influence of laser wavelength on particle size. Appl. Surf. Sci. 202, 80–85.

Vaucher, S., Fielden, J., Li, M., Dujardin, E., Mann, S., 2002. Molecule-based magnetic nanoparticles: synthesis of cobalt hexacyanoferrate, cobalt pentacyanonitrosyl ferrate and chromium hexacyanochromate coordination polymers in water-in-oil microemulsions. Nano Lett. 2, 225–229.

Voigt, A., Adityawarman, D., Sundmacher, K., 2005. Size and distribution prediction for nanoparticles produced by microemulsion precipitation: a Monte-Carlo simulation study. Nanotechonology 16, 429–434.

Wang, L.N., Zhang, Y., Muhammed, M., 1995. Synthesis of nanophase oxalate precursors of YBaCuO superconductor by coprecipitation in microemulsions. J. Mater. Chem. 5, 309–314.

Wanzhong, Z., Xueliang, Q., Jianguo, C., 2006. Synthesis and characterization of silver nanoparticles in AOT microemulsion system. Chem. Phys. 330, 495–500.

Wilcoxon, J.P., Provencio, P.P., 1999. Use of surfactant micelles to control the structure phase of nanosize iron clusters. J. Phys. Chem. B 103, 9809–9812.

Wu, M.L., Chen, D.H., Huang, T.C., 2001a. Synthesis of Au/Pd bimetallic nanoparticles in reverse micelles. Langmuir 17, 3877–3883.

Wu, M.L., Chen, D.H., Huang, T.C., 2001b. of Pd/Pt bimetallic nanoparticles in water/AOT/isooctane microemulsions. J. Colloid. Interf. Sci. 243, 102–108.

Wu, Z., Zhang, J., Benfield, R.E., Ding, Y., Grandjean, D., Zhang, Z., Ju, X., 2002. Structure and chemical transformation in cerium oxide nanoparticles coated by surfactant cetyltrimethylammonium bromide (CTAB): an X-ray absorption spectroscopy study. J. Phys. Chem. B 106, 4569–4577.

Xike, T., Jinbo, F., Zhenbang, C., Yang, L., Dongyue, A., 2005. Synthesis and characterization of amoxicillin nanostructures. Nanomed.: Nanotech. Biol. Med. 1, 323–325.

Xu, S., Li, Y., 2003. Different morphology at different reactant molar ratios: synthesis of silver halide low-dimensional in microemulsions. J. Mater. Chem. 13, 163–165.

Yashima, M., Falk, L.K.L., Palmqvist, A.E.C., Holmberg, K., 2003. Structure and catalytic properties of nanosized alumina supported platinum and palladium particles synthesized by reaction in microemulsion. J. Colloid. Interf. Sci. 268, 348–356.

Yener, D.O., Giesche, H., 2001. Synthesis of pure and manganese-nicel and zinc-doped ferrite particles in water-in-oil microemulsions. J. Am. Ceram. Soc. 84, 1987–1995.

Yu, K.M.K., Yeung, C.M.Y., Thompsett, D., Tsang, S.C., 2003. Aerogel-coated metal nanoparticle colloid as novel entities for the synthesis of defined supported metal catalysis. J. Phys. Chem. B 107, 4515–4526.

Zaheer, Z., Malik, M.A., Al-Nowaiser, F.M., Khan, Z., 2010. Preparation of silver nanoparticles using tryptophan and its formation mechanism. Colloid. Surf. B: Biointerf. 81, 587–592.

Zhand, R., Gao, L., 2002. Preparation of nanosized Titania by hydrolysis of alkoxide titanium in micelles. Mater. Res. Bull. 37, 1659–1666.

Zhang, D., Qi, L., Ma, J., Cheng, H., 2002. Formation of crystalline nanosized Titania in reverse micelles at room temperature. J. Mater. Chem. 12, 3677–3680.

Zhang, X., Chan, K.Y., 2003. Water-in-oil microemulsions synthesis of platinum-ruthenium nanoparticles, their characterization and electrocatalytic properties. Chem. Mater. 15, 451–459.

Zhang, X., Chan, K.Y., 2002. Microemulsion synthesis and electrocatalytic properties of platinum–cobalt nanoparticles. J. Mater. Chem. 12, 1203–1206.

Zhong-min, O., Hiroshi, Y., Keisaku, K., 2007. Preparation and optical properties of organic nanoparticles of porphyrin without self-aggregation. J. Photochem. Photobio. A: Chem. 189, 7–14.